

# Ice-core palaeoclimate records in tropical South America since the Last Glacial Maximum

Lonnie G. Thompson<sup>1,2,\*</sup>, Ellen Mosley-Thompson<sup>1,3</sup> and Keith A. Henderson<sup>1,2</sup>

<sup>1</sup>Byrd Polar Research Center, The Ohio State University, Columbus, Ohio 43210, USA

<sup>2</sup>Department of Geological Sciences, The Ohio State University, Columbus, Ohio 43210, USA

<sup>3</sup>Department of Geography, The Ohio State University, Columbus, Ohio 43210, USA

Thompson L. G., Mosley-Thompson E. and Henderson, K. A. 2000. Ice-core palaeoclimate records in tropical South America since the Last Glacial Maximum. *J. Quaternary Sci.*, Vol. 15, pp. 377–394. ISSN 0267-8179.

Received 11 October 1999; Revised 10 January 2000; Accepted 18 January 2000

**ABSTRACT:** Ice-core records spanning the last 25 000 yr from the tropical Andes of South America are reviewed. These records from Quelccaya, Huascarán and Sajama present a high temporal resolution picture of both the Late Glacial Stage (LGS) and the Holocene climatic and environmental conditions in the South American Andes. Late Glacial Stage conditions at high elevations appear to have been cooler than today, although the magnitude of the inferred cooling differs with the particular proxy used (e.g. snowline depression, pollen, ice cores). Insoluble dust and anion concentrations in the ice cores reveal that LGS hydrological conditions in the tropics (9°S) were much drier than today, whereas in the subtropics (18°S) LGS conditions were much wetter. This probably reflects the migration of the tropical Hadley Cell in response to a different meridional temperature gradient. Low nitrate concentrations in the LGS ice from both Huascarán and Sajama suggest that the Amazon Basin forest cover may have been much less extensive. Discussed is the conundrum surrounding the use of  $\delta^{18}\text{O}$  as a palaeothermometer in the tropics, where temperatures exhibit little seasonal variation yet the ice-core records suggest that  $\delta^{18}\text{O}$  records temperature variations on decadal to millennial time-scales. Finally evidence is presented for a strong twentieth century warming. Copyright © 2000 John Wiley & Sons, Ltd.

**KEYWORDS:** palaeoclimate; ice cores; Holocene; Last Glacial Maximum; Younger Dryas.

**JQS**  
Journal of Quaternary Science

## Introduction

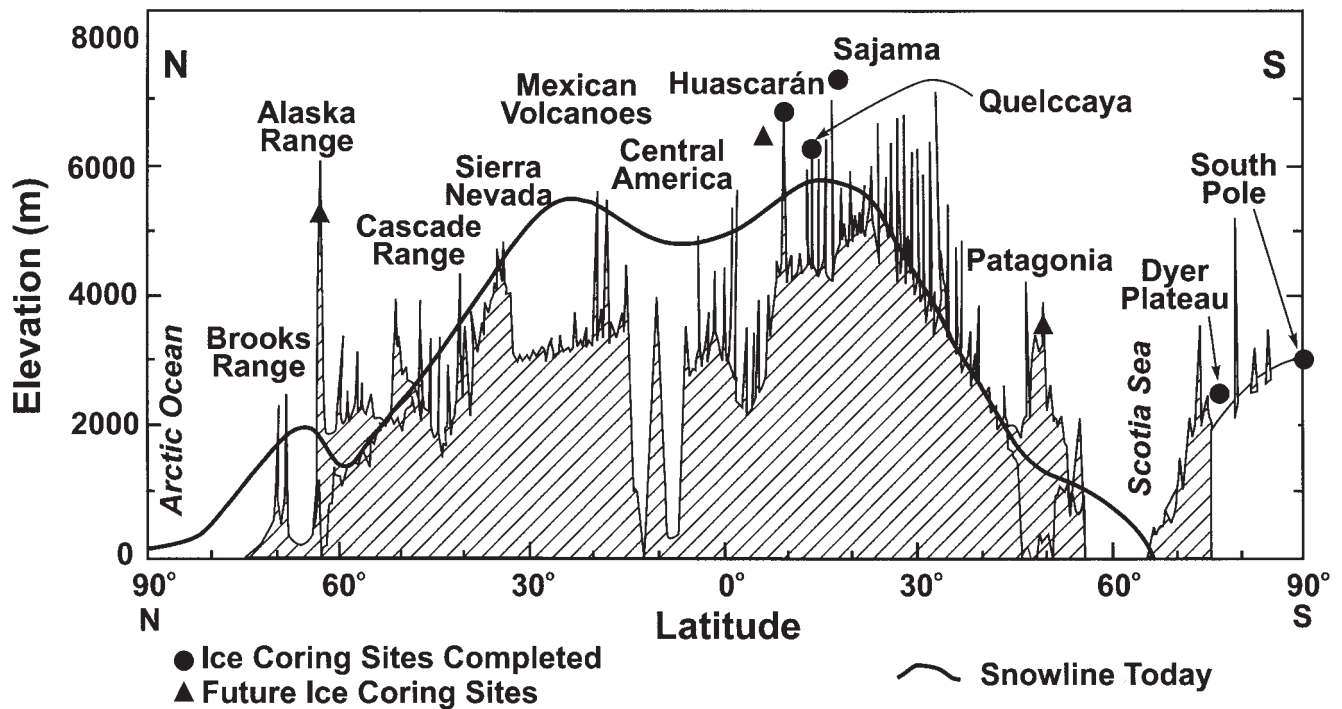
The development of a programme to retrieve ice-core palaeoclimatic histories in the South American Andes was a natural extension of the successful ice-coring projects in Greenland and Antarctica. Polar ice-cores have contributed to Late Quaternary climate histories with much higher resolution than were previously available from existing sedimentary sequences. In the last 15 yr tropical and subtropical ice-cores have begun to contribute significantly to our understanding of global-scale climate variability by providing multifaceted, high temporal resolution, and in some cases lengthy palaeohistories. In addition, tropical and subtropical ice-fields exist closer to the centres of action for several

major components of the climate system, such as the El Niño-Southern Oscillation (ENSO) and the Asian monsoonal regime. The ENSO and monsoons are highly variable components of the climate system, with the potential to affect the lives of most of the Earth's inhabitants, either directly or indirectly. Therefore, knowledge of the history of their variability, including the range of potential impact, is important for ongoing modelling efforts attempting to predict how these systems may change under the anticipated anthropogenic warming in the twenty-first century.

The first long tropical ice-core was recovered in 1983 from the Quelccaya ice-cap (Fig. 1) in the southern Andes of Peru (13.93°S; 70.83°W). Interestingly, the idea of drilling these tropical cores was born nearly a decade earlier in 1974 when Lonnie Thompson accompanied John Mercer and John Ricker to Quelccaya to collect basic, preliminary glaciological information about the site. The excellent preservation of annual layers visible along the vertical margins of Quelccaya (see cover of *Science* 203, 1979) promised an annually resolved ice-core record. The successful recovery of the Quelccaya cores required the development of a light-weight, portable solar powered drilling system. Although this new drilling system was conceived in 1979, it was not until 1983 that it was used to recover two cores (158.4 m and

\* Correspondence to: Dr. L. G. Thompson, Byrd Polar Research Center, 108 Scott Hall, 1090 Carmack Road, Columbus OH 43210, USA.  
E-mail: thompson.3@osu.edu

Contract grant sponsor: National Science Foundation (USA)  
Contract grant number: ATM89-16635  
Contract grant sponsor: National Oceanic and Atmospheric Administration  
Contract grant number: NA16RC0525-01, NA76GP0025



(modified from Broecker and Denton, 1990)

**Figure 1** Shown are the locations of completed and planned ice coring sites along the North and South American Cordillera along with current snow lines. This figure was modified from Broecker and Denton (1990) and provided originally to them by Dr Steven Porter.

163.3 m long) to bedrock from the Quelccaya summit. Although the Quelccaya records extend back only 1.5 millennia, they have provided a plethora of information about the climate history of that region (Thompson *et al.*, 1984a, 1984b, 1985, 1986, 1988). The annual data from the Quelccaya ice-cores are available electronically at the National Geophysical Data Center (<ftp://ftp.ngdc.noaa.gov/paleo/icecore/trop/quelccaya>).

The successful Quelccaya drilling demonstrated the feasibility of recovering ice-core histories from high elevation, low-latitude ice fields. In subsequent years palaeoclimate histories have been attained from the Dundee (Thompson *et al.*, 1989) and Guliya (Thompson *et al.*, 1997) ice-caps in China as well from two additional sites in the tropical South American Andes, Huascarán (Peru) and Sajama (Bolivia). The latter two records extending back into the Late Glacial Stage (LGS) and the shorter record from the Quelccaya ice-cap are highlighted in this paper.

## Late Glacial Stage climate as revealed by ice cores

Glacial geological evidence throughout the Andes attests to the expansion of mountain glaciers during the LGS for which Clapperton (1993a) provides an excellent synthesis. The pioneering work of the late John H. Mercer, Steve Porter and Herbert Wright, among others, suggested that glaciers in the South American Andes expanded and contracted in virtual synchronicity with the Northern Hemisphere ice sheets. Another key observation of LGS conditions is a consistent snowline depression of 900 to 1000 m throughout the Andes (Herd and Naeser, 1974; Porter, 1979; Broecker and Denton, 1990; Rodbell, 1992; Klein *et al.*, 1995). It has

been suggested that this snowline lowering may have been globally consistent (Rind and Peteet, 1985), dropping nearly the same elevation in the tropics as in mid-latitudes of both hemispheres. However, the dating of glacial deposits is imprecise and synchronicity remains speculative. Seltzer (1990) points out that phases of glaciation must be correlated not only to colder conditions but to a substantial increase in precipitation. Movement of the Intertropical Convergence Zone (ITCZ) in response to a large-scale temperature forcing (e.g. cooling) would result in the migration of centres of wet and dry conditions so that glaciers in one region might expand and whereas those in another might contract.

In the last decade, diverse proxy indicators have provided a more comprehensive view of LGS cooling in the tropics and subtropics. The location of these archives has ranged in altitude from the ocean surface (e.g. coral records) to the mountain peaks (e.g. ice-core records). Recent alkenone data (Bard *et al.*, 1997; Wolff *et al.*, 1998) suggest temperatures at sea-level that are more consistent with the CLIMAP (1976, 1981) reconstructions. Other evidence, such as the coral records of Guilderson *et al.*, (1994) and Beck *et al.*, (1997), along with noble gases from groundwater (Stute *et al.*, 1995), marine sediment pore-fluids (Schrag *et al.*, 1996), and pollen (Colinvaux *et al.*, 1996), all suggest climatic conditions cooler than the 1° to 2°C drop in tropical sea-surface temperatures established by CLIMAP. Recent ice-cores from Huascarán (Peru) and Sajama (Bolivia) present a high temporal resolution picture of both LGS and Holocene climatic and environmental conditions at high elevation in the South American Andes, and suggest that LGS conditions there were cooler by more than 1 or 2°C.

## The Huascarán (Peru) ice-core record

In 1993 two ice cores were drilled to bedrock on the col (6048 m a.s.l.) of Huascarán, Peru (9.11°S; 77.61°W). These

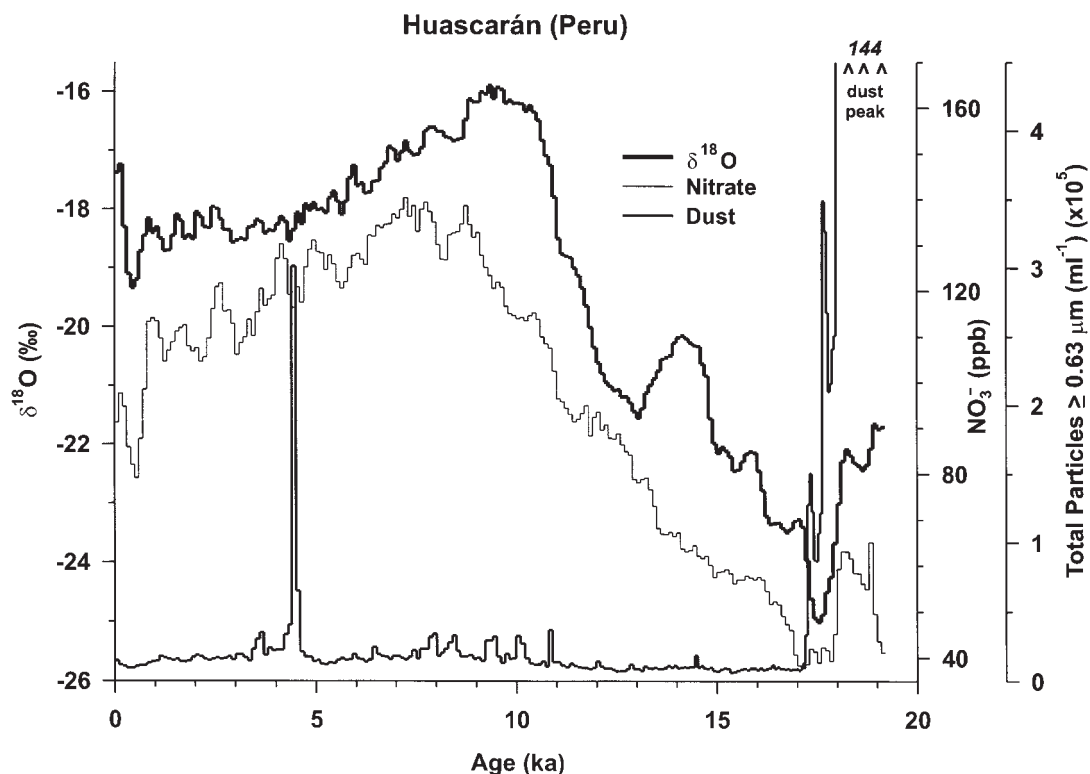
cores have provided the first high temporal resolution ice-core record of the climatic and environmental conditions in the Andes extending back into the LGS approximately 20 000 yr BP (Thompson *et al.*, 1995). Since that publication, the dating of the Huascarán cores has been revised using a combination of methods. These include: layer counting over the most recent 270 yr, measurements of the  $\delta^{18}\text{O}_{\text{air}}$  in Core 2 bubbles (Sowers, unpublished data), and the use of a two-parameter thinning model (Thompson *et al.*, 1990) for Core 1. Similar Holocene histories were produced for the two cores by these various methods despite differences in the thinning behaviour in the deepest ice between the two sites. Further, both Huascarán core records include the entire deglaciation sequence and confirm a distinct climatic reversal similar to the Younger Dryas cool phase so prominent in the North Atlantic region. As demonstrated in Thompson *et al.* (1995), the fluctuations in Huascarán  $\delta^{18}\text{O}$  correspond well with variations in the planktonic foraminifer  $\delta^{18}\text{O}$  from the marine core SU81-18 (near Portugal; Bard *et al.*, 1987), and thus the corrected radiocarbon ages from that work were used to calibrate the Huascarán age scale from ca. 12 to 19 kyr ago. The  $\delta^{18}\text{O}$  record from Huascarán contributes to a growing body of evidence that LGS conditions in the Andes were much cooler (perhaps as much as 8°C) than during the Holocene. In contrast, the magnitude of LGS cooling at lower elevations, near sea-level, is still unresolved. The Barbados corals (Guilderson *et al.*, 1994) and noble gases in groundwater (Stute *et al.*, 1995) suggest greater cooling than foraminifer (Wolff *et al.*, 1998) and alkenone records (Bard *et al.*, 1997), which are more consistent with CLIMAP (1981).

Figure 2 illustrates 100-yr averages of  $\delta^{18}\text{O}$  along with concentrations of nitrate and insoluble dust for the last 20 000 yr. The most notable features are the 6.3‰ depletion of  $\delta^{18}\text{O}$ , a 200-fold increase in insoluble dust, and the two- to three-fold decrease in  $\text{NO}_3^-$  in the ice inferred to be of

LGS age. The 6.3‰ depletion of  $\delta^{18}\text{O}$  in Huascarán LGS ice, relative to the overlying Holocene ice, is very comparable to the correlative 6‰ depletion in LGS ice from Dome C, Antarctica (Thompson and Mosley-Thompson, 1981; Petit *et al.*, 1981) and exceeds the 5.1‰ depletion in the GISP2 core (Grootes *et al.*, 1993). Here we refrain from applying a simple  $\delta^{18}\text{O}$ -temperature relationship, such as is used in the polar regions (Dansgaard and Oeschger, 1989), to the 6.3‰ depletion in Huascarán as such a relationship has not been quantified in this region. However, we do interpret this isotopic depletion as a reflection of significant cooling and we defend this interpretation later in this paper. The Huascarán results support the emerging view of much colder LGS conditions in the tropics, particularly over land and at higher elevations, than originally inferred from reconstructions of sea-surface temperatures (CLIMAP, 1976, 1981).

Additional palaeoenvironmental information about LGS conditions is preserved in the Huascarán cores. The insoluble dust concentrations (Fig. 2) in LGS ice are very high, nearly 200 times those in Holocene ice. This increase in atmospheric turbidity during the glacial stage was first documented in polar ice-cores (see review by Mosley-Thompson and Thompson, 1994) as well as in the LGS ice from the Dunde Ice Cap, China (Thompson *et al.*, 1989). The extreme dustiness in Huascarán LGS ice is consistent with climate reconstructions for tropical South America and suggests lower atmospheric humidity and precipitation, as well as a possible reduction of forest and grass cover (Clapperton, 1993b). Clapperton estimated that up to 25% of South America was covered by aeolian deposits such as sand dunes and loess (Fig. 3).

Figure 2 also illustrates that the concentration of nitrate ( $\text{NO}_3^-$ ) is reduced by three- to four-fold in the glacial stage ice. Although the sources of atmospheric  $\text{NO}_3^-$  are not well defined, recent evidence indicates that tropical rain forests and forest soils may be a major source of active atmospheric



**Figure 2** Shown are the 100-yr averages of  $\delta^{18}\text{O}$  and concentrations of nitrate ( $\text{NO}_3^-$ ) and insoluble particles (dust with diameters  $\geq 0.63 \mu\text{m ml}^{-1}$ ) from the last 20 000 yr of the Huascarán (Peru) ice-core. This figure was modified from Thompson *et al.* (1995).

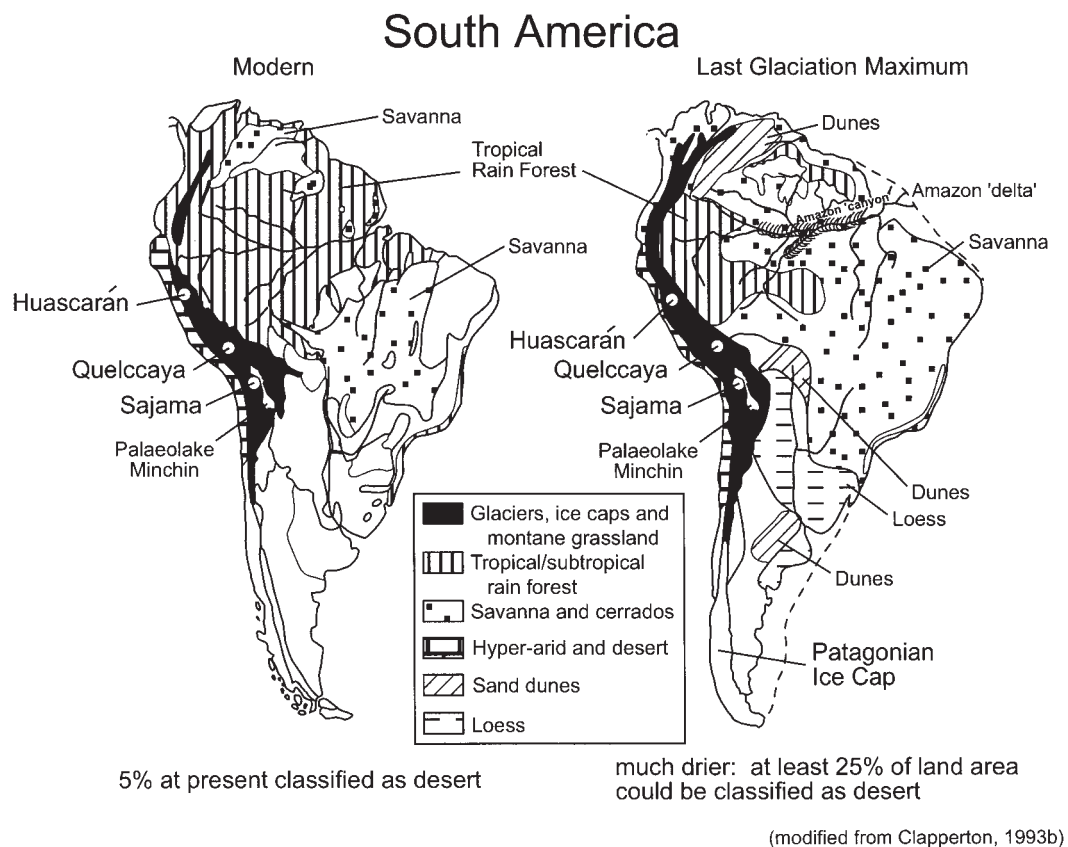


**Figure 3** This sketch illustrates Clapperton's inferred changes in major vegetation types from the Last Glacial Maximum to the present. Also shown are selected geomorphological features along with the locations of the Quelccaya, Huascarán, and Sajama ice-core drilling sites. This figure is adapted from Clapperton (1993b).

nitrogen species such as  $\text{NO}$  and  $\text{NH}_3$ , which serve as precursors for  $\text{NO}_3^-$  and  $\text{NH}_4^+$  that occur as aerosols (Robertson and Tiedje, 1988; Talbot *et al.*, 1988). Pollen concentrations in five selected core sections (two late Holocene, two early Holocene and one LGS) reveal abundant pollen in late Holocene ice, less pollen in the early Holocene samples and virtually no pollen in the LGS sample. Thus, the pollen record from Huascarán supports the other ice-core data indicating a cold, sparsely vegetated LGS environment where pollen productivity was low and montane vegetation was displaced downward (Thompson *et al.*, 1995; Bush *et al.*, 1990). Figure 3 illustrates the vegetation and surface cover inferred for both modern and glacial stage conditions (Clapperton, 1993b). The nature of the vegetation response in the Amazon is not clear-cut, and probably not simple to ascertain. Recent pollen studies from the Amazon Fan suggest little glacial–interglacial change in vegetation along the riparian zone and only modest expansion of the savanna at the expense of the rain forest (Haberle and Maslin, 1999). Conversely, unweathered plagioclase in glacial stage sediments of the Amazon Fan are interpreted as indicative of a drier climate with a reduced forest cover in the Amazon (Damuth and Fairbridge, 1970). The reduction of forest cover and expansion of savannas, coupled with the increased abundance of aeolian deposits during the LGS, are consistent with the Huascarán  $\delta^{18}\text{O}$ , dust, nitrate and pollen histories. The Huascarán record reveals a prominent climate reversal just before the final warming to early Holocene conditions (Fig. 2). Thompson *et al.* (1995) suggest that this cool phase may be correlative with the Younger Dryas cooling prominent around the North Atlantic (Petee, 1995). At the time of their publication, this reversal to cooler conditions was unconfirmed in the South American Andes.

The original time-scale for Huascarán was not derived independently, but was tied to an AMS  $^{14}\text{C}$  dated  $\delta^{18}\text{O}$  (*Globigerina bulloides*) record from a marine core off the coast of Portugal (Bard *et al.*, 1987). However, the well-dated Sajama core discussed in the next section confirms that this deglaciation climate reversal was indeed prominent in the Andes. This climate event is now emerging as a consistent feature of the global deglaciation sequence, although the timing, and hence its interhemispheric synchronicity, remains under discussion (Bard *et al.*, 1997; Steig *et al.*, 1998; White and Steig, 1998).

Holocene climatic and environmental conditions in the tropical Andes are preserved in the Huascarán ice-cores, presented on the revised time-scale in Fig. 2. The new chronology indicates that the isotopically warmest ice was deposited in the early Holocene and since then conditions in the Andes have steadily cooled. Superimposed upon this steady temperature decline are minor centennial-scale  $\delta^{18}\text{O}$  oscillations. As conditions warmed during the transition from LGS to Holocene conditions the increase in atmospheric nitrate lagged the atmospheric warming by several millennia. The early Holocene lag in the increasing  $\text{NO}_3^-$  concentrations may reflect successional vegetation changes, possibly requiring up to 2000 yr for maximum regrowth of the tropical rain forests of Amazonia after their marked reduction (Fig. 3) during the LGS. In the last half of the Holocene  $\delta^{18}\text{O}$  and  $\text{NO}_3^-$  have varied more synchronously, reaching their coolest and lowest (respectively) values during the most recent Neoglacial (the Little Ice Age). In the last 200 yr both  $\text{NO}_3^-$  and  $\delta^{18}\text{O}$  have increased markedly and twentieth century  $\delta^{18}\text{O}$  values are the most enriched (warmest) of the last 6000 yr. Additional evidence for and implications of this recent warming will be addressed in the last section of this paper.

## The Sajama (Bolivia) ice-core history

Four cores, two to bedrock, were retrieved in 1997 (Thompson *et al.*, 1998) from the summit (6542 m a.s.l.) of the Sajama ice-cap (18°06'S; 68°58'W). The ice cap completely covers the top of the extinct Sajama Volcano located on the northern boundary of a large desert on the Altiplano. The Altiplano, the world's second largest plateau (Clapperton, 1993a), has a mean elevation of 3700 m and contains a northern and southern basin. The northern basin is occupied by Lake Titicaca whereas the southern basin contains shallow saline lakes and salt flats such as the Salar de Uyuni, the world's largest salt flat (ca. 12 500 km<sup>2</sup>). Precipitation is low and quickly evaporates leaving salt crusts in much of the Poopó Basin, which also contains hypersaline Lake Poopó. Like Huascarán and Quelccaya, the dominant moisture source for Sajama is the Atlantic, as water vapour is advected from the east and northeast over the Amazon Basin.

Figure 4 presents the Sajama  $\delta^{18}\text{O}$ ,  $\text{NO}_3^-$  and dust histories for the last 20 000 yr shown in similar fashion as for Huascarán (Fig. 2). The Sajama cores are unique as they contain intact insects, insect fragments and polylepis bark fragments that allowed AMS  $^{14}\text{C}$  dating to constrain the time-scale. At a depth in the core 1.5 m above the bedrock, sufficient plant material for AMS radiocarbon dating was found. The sample was divided into two portions that gave dates of  $24\,950 \pm 430$   $^{14}\text{C}_{\text{cal}}$  yr (Lawrence Livermore National Laboratory) and of  $24\,020 \pm 140$   $^{14}\text{C}_{\text{cal}}$  yr (Woods Hole Oceanographic Institution) ago. The calibration method of Stuiver and Reimer (1993) and Bard (1998) was used to convert  $^{14}\text{C}$  yr to  $^{14}\text{C}_{\text{cal}}$  (calendar) yr. These dates confirm that the near-basal ice on Sajama is of LGS age. No other datable material was found in the Late Glacial or early Holocene ice, but additional datable material was obtained in ice ranging in age from ca. 150 to 5610  $^{14}\text{C}_{\text{cal}}$  yr ago.

Other dating tools used on the Sajama cores include layer counting in the upper sections, identification of the Huaynaputina volcanic ash (AD 1600), and correlating the  $\delta^{18}\text{O}_{\text{atm}}$  data from Sajama with an analogous record from the GISP2 core that was dated by layer counting (Alley *et al.*, 1997). The  $\delta^{18}\text{O}_{\text{ice}}$  records from Sajama and GISP2 contain similar sequences of major and minor events (Fig. 5). Assuming that these  $\delta^{18}\text{O}_{\text{ice}}$  features are temporally synchronous, 14 matching points with the GISP2 core were identified between 104 and 123 m in Sajama, thus further constraining the time-scale between 11 and 19 kyr (Fig. 5). Details of the Sajama time-scale development are presented by Thompson *et al.*, (1998) and the  $^{14}\text{C}_{\text{cal}}$  dates and  $\delta^{18}\text{O}_{\text{atm}}$  match points are shown in Fig. 5 (top profile). Because the time interval subject to GISP2 cross-dating is bounded by well-determined ages, the matching itself is not crucial to the millennial-scale age dating of the core. Further, the final age scale dictates that a sharp decrease in accumulation occurred precisely at the beginning of the Holocene (ca. 10 kyr ago), which produces a coherent picture with the palaeoleak chronologies presented below.

The Sajama  $\delta^{18}\text{O}$  record (Fig. 4), coupled with that from Huascarán, suggests very cool LGS conditions throughout the tropical and subtropical Andes. Table 1 illustrates that the LGS isotopic depletion of 5.4‰ on Sajama is comparable to that found in contemporaneous ice-cores from Greenland, Antarctica, China and Peru. All the ice cores in Table 1 have similar isotopic depletions between both the LGM and modern (last 1000 yr) ice and LGM and Early Holocene ice. Coupled with records from other previously mentioned archives (e.g. snow-line depression, noble gases from groundwater in the Amazon Basin, and corals) the Sajama and Huascarán ice-core records suggest an even greater LGS tropical cooling than the 2–3°C cooling inferred from recent foraminiferal (Wolff *et al.*, 1998) and alkenone reconstructions (Bard *et al.*, 1997).

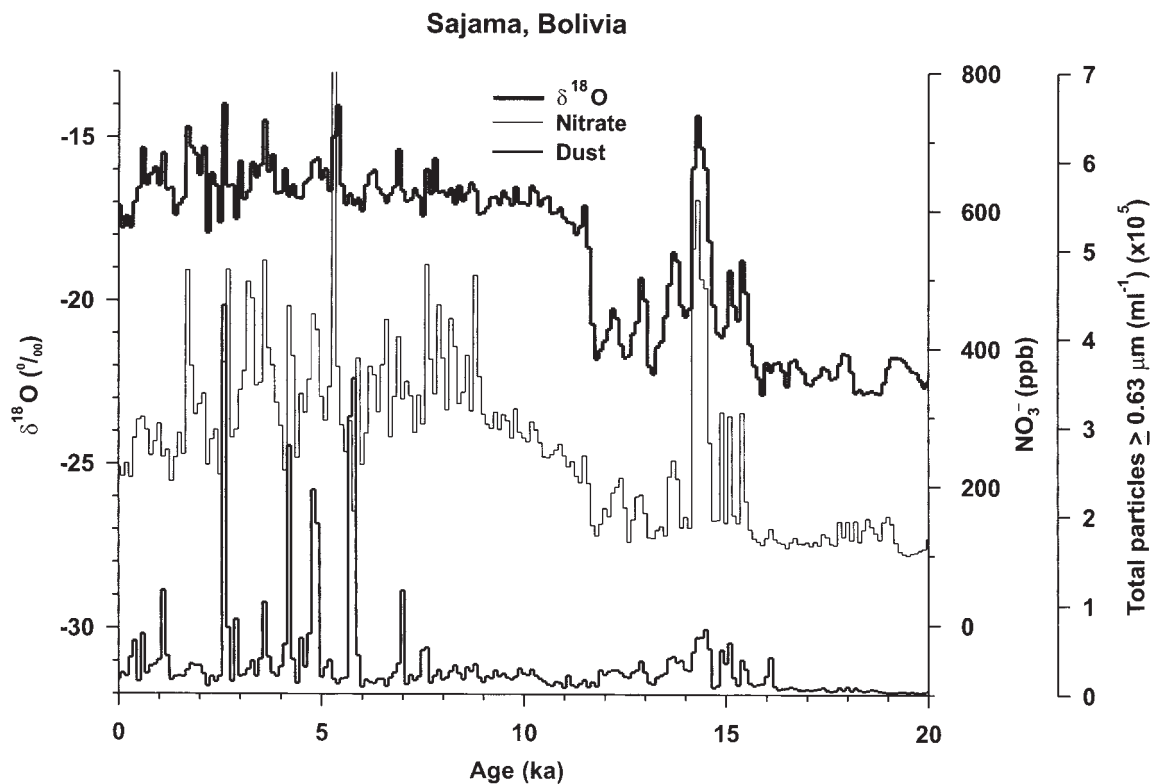


**Figure 4** Shown are the 100-yr averages of  $\delta^{18}\text{O}$  and concentrations of nitrate ( $\text{NO}_3^-$ ) and insoluble particles (dust with diameters  $\geq 0.63 \mu\text{m ml}^{-1}$ ) from the last 20 000 yr of the Sajama (Bolivia) ice-core. This figure was modified from Thompson *et al.* (1998).

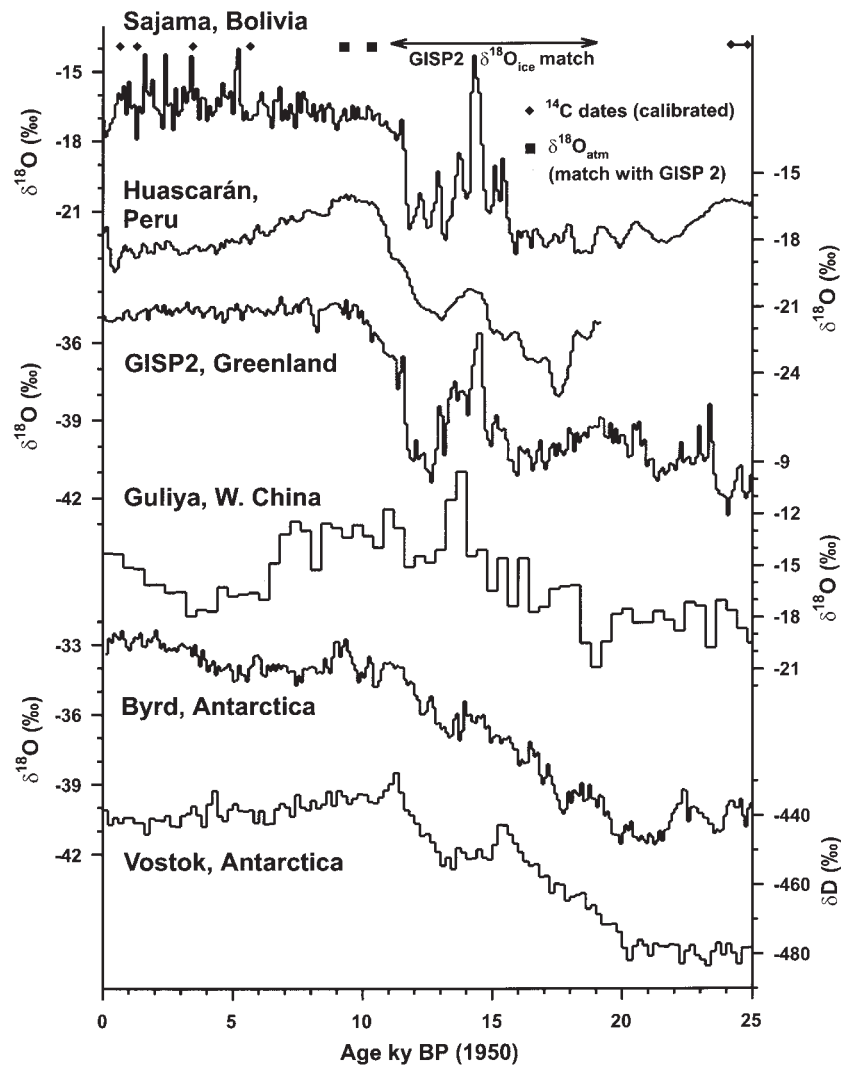


**Figure 5** These  $\delta^{18}\text{O}$  and  $\delta\text{D}$  histories illustrate the global extent of the LGS and the deglaciation climate reversal (cooling) for the last 25 000 yr as preserved in Sajama and Huascarán, GISP2 in Greenland (Grootes *et al.*, 1993), Guliya in western China (Thompson *et al.*, 1997), and Byrd Station (Johnsen *et al.*, 1972) and Vostok (Jouzel *et al.*, 1987) in Antarctica. All records are 100-yr averages except Vostok (200-yr averages) and Guliya (400-yr averages). Shown along the top are the  $^{14}\text{C}_{\text{cal}}$  dates, the  $\delta^{18}\text{O}_{\text{atm}}$  match points and the time interval over which  $\delta^{18}\text{O}_{\text{ice}}$  was matched to that in the GISP2 core. This figure was modified from Thompson *et al.* (1998).

**Table 1** The average  $\delta^{18}\text{O}$  values for various time intervals and for different ice-cores are compared.  $\delta\text{D}$  was measured for Vostok and the comparable  $\delta^{18}\text{O}$  values ( $\delta\text{D} = 8\delta^{18}\text{O} + 10$ ) are shown in parentheses. These records are shown in Fig. 5 and the pertinent references are cited in the text

	Modern (0–1 ka)	Early Holocene (EH) (6.8–10.0 ka)	Last Glacial Maximum (LGM) (18.0–21.2 ka)	MODERN – LGM (‰)	EH – LGM (‰)
Sajama (Bolivia)	–16.8	–16.7	–22.1	5.4	5.4
Huascarán (Peru)	–18.5	–16.6	–22.9	4.4	6.3
GISP 2 (Greenland)	–35.0	–34.6	–39.7	4.7	5.1
Guliya (W. China)	–14.4	–13.1	–18.5	4.1	5.4
Byrd (Antarctica)	–32.8	–33.9	–40.5	7.6	6.6
Vostok (Antarctica)	–441 (–56.4)	–436 (–55.7)	–472 (–60.2)	3.9	4.5
Vostok (21–24.2 ka)			–479 (–61.1)	4.8	5.4

The Sajama and Huascarán records contain some important differences, particularly in their dust and nitrate concentrations, that reflect their dissimilar environmental settings. Unlike Huascarán and the polar ice-cores, Sajama does not contain elevated concentrations of dust at the height of the LGS cooling. This lack of LGS dustiness reflects

Sajama's location in the subtropics, where large regional palaeolakes existed (Minchin, 1882; Clapperton *et al.*, 1997). At the same time, nitrate concentrations were low and  $\delta^{18}\text{O}$  was depleted, suggesting that conditions from 20 ka to 15.5 ka were cold and moist in this region. At 15.5 ka the climate warmed abruptly and became drier as reflected in

the increasing deposition of soluble aerosols (factor of three to five for  $\text{NO}_3^-$ , five to seven for  $\text{Cl}^-$  and  $\text{SO}_4^{2-}$ ) and insoluble dust. This progressive and oscillating warming culminated at ca. 14.3 ka with the isotopically warmest period in the last 20 ka. The aridity at this time is evident in the high concentrations of insoluble dust and all three major anions ( $\text{Cl}^-$ ,  $\text{SO}_4^{2-}$ , and  $\text{NO}_3^-$ ; see fig. 6 in Thompson *et al.*, 1998) that characterise soluble aerosol species.

This interstadial (warming) event terminated abruptly at ca. 14 ka, when climate quickly reversed to much cooler conditions similar to those attributed to the North Atlantic Younger Dryas (YD) stadial (Peteet, 1995). Thompson *et al.*, (1998) refer to this event as the DCR (deglaciation climate reversal) to distinguish it from the YD. On Sajama,  $\delta^{18}\text{O}$  decreases from the enriched values of the previous interstadial (14 to 14.3 ka) by an amount comparable to that in Greenland (Grootes *et al.*, 1993) ice-cores (5.2‰ versus 5.3‰). During the DCR, environmental conditions in this region of the Altiplano appear similar to those prevailing there at the LGM. The colder temperatures were accompanied by higher net precipitation and high lake stands, as inferred from decreases in aerosol concentrations. Palynological and glacial geological studies elsewhere in the Andes (Seltzer, 1992, 1994), along with earlier water budget studies (Hastenrath and Kutzbach, 1985; Kessler, 1985) confirm that the initial rise of Tauca Lake did not result from melting glaciers, but from a precipitation increase over the Altiplano. During the DCR the dust concentrations at both Sajama and Huascarán show a slight decrease, consistent with dust concentrations in Antarctic cores (Thompson and Mosley-Thompson, 1981), but in contrast to the significant increase of dust in the YD ice of the Greenland ice-cores (Taylor *et al.*, 1993; Hammer *et al.*, 1985). These differences suggest that atmospheric dust loading during the YD was restricted to the Northern Hemisphere, probably the product of the glacial flour generated along the fluctuating margins of the large Northern Hemisphere ice sheets. In the Andes the colder conditions of the DCR persisted until 11.5 ka, when

warming occurred in just a few centuries and marked the onset of the Holocene (Fig. 4).

Clapperton (1993a, p. 454) suggested that the limited sedimentary, palynological and glacial geomorphological data were suggestive of, but not yet persuasive for, a distinct climate reversal in the Andes from 12 500 to 10 000  $^{14}\text{C}$  yr BP (14 700–11 440 cal. yr BP). The Sajama and Huascarán  $\delta^{18}\text{O}$  histories confirm this climate reversal (14 to 11.5 ka) in the Peruvian and Bolivian Andes. In addition, confirmation of the 2500-yr-long DCR also solves the 'Mercer Problem', as Clapperton (1993a) referred to John Mercer's view that the Younger Dryas cooling was restricted to northwestern Europe. Mercer (1969) concluded that Patagonian glaciers attained their Holocene minima by 11 000  $^{14}\text{C}$  yr BP (13 000 cal. yr BP). However, he later found evidence (Mercer, 1984) for a distinct readvance of Peruvian glaciers at ca. 11 460  $^{14}\text{C}$  yr BP (13 400 cal. yr BP) and concluded that the readvance had pre-dated the onset of the YD (13 000 cal. yr BP) by ca. 500 yr. In fact, this late glacial readvance of Peruvian and Ecuadorian glaciers (Clapperton, 1993c) is entirely consistent with, and undoubtedly in direct response to, the climate reversal beginning at 14 000 cal. yr BP over much of the tropical and subtropical South American Andes.

At the termination of the DCR, lakes gradually became desiccated and this drying continued well into the Holocene. This is supported by the soluble and insoluble aerosol concentrations that remained low until ca. 9 ka, when abrupt increases in aerosol deposition signalled the final drying of the extensive flat-bottomed lakes. The insoluble dust concentrations in the Holocene ice on Sajama are eight times that in the LGM ice and results from a combination of increased local volcanic activity, an increase in the surface area of dust exposed by elevated Holocene snow lines, and decreased accumulation from early Holocene to ca. 3.4 ka. The high concentrations of soluble species (fig. 6 in Thompson *et al.*, 1998) and insoluble dust indicate that the lake levels on the Altiplano were low from 9 ka (lagging the accumulation

### Isotope Fractionation Model involving Amazon Basin hydrology

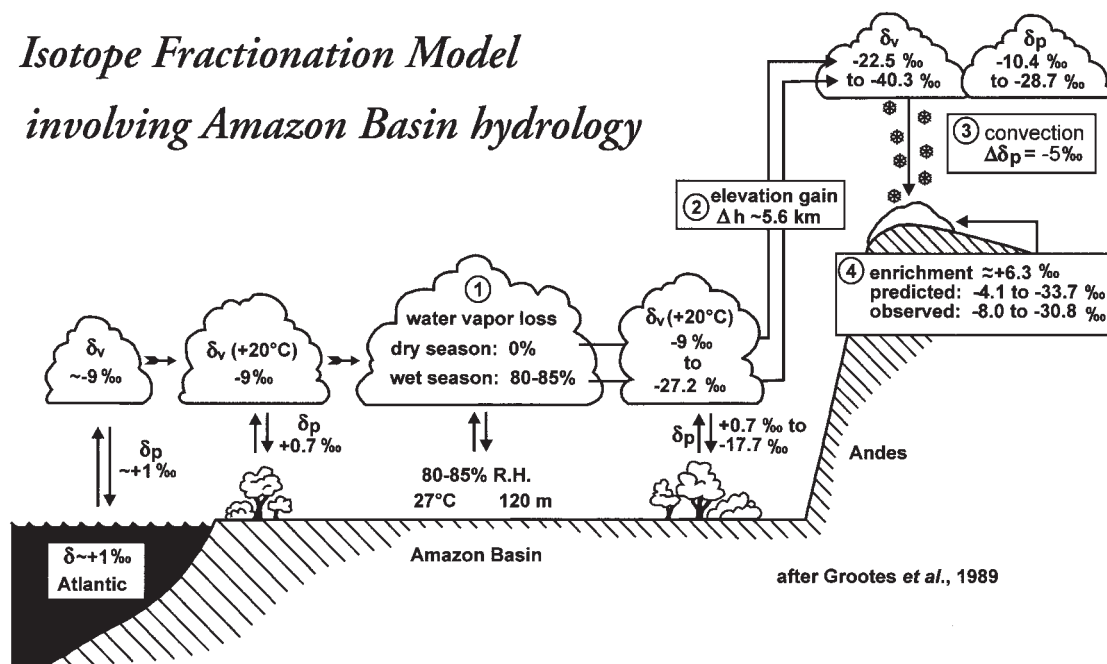


**Figure 6** This schematic traces the  $\delta^{18}\text{O}$  composition of the water vapor and precipitation along a transect from the Atlantic Ocean to the top of the Andes (Quelccaya ice cap). Each of the four steps shown is discussed in the text. This figure was modified from Grootes *et al.* (1989).

decrease by ca. 2.5 kyr) to 3 ka. Water levels in Lake Titicaca in the northern basin were also low from ca. 7.7 ka to 3.5 ka (Wirrman and Mouguiart, 1995). The decrease of aerosols from ca. 3 ka to the present reflects increasing accumulation in the region (Thompson *et al.*, 1998, fig. 6), consistent with slightly higher levels in Lake Titicaca (Abbott *et al.*, 1997).

The palaeoclimate record preserved in the Sajama ice-cores strongly reflects the waxing and waning of the palaeo-lakes, a dominant feature of the Altiplano (Minchin, 1882). The presence or absence of these lakes reflect regional changes in the climate system. On the Altiplano, cold periods were generally wet and so glaciers in the cordilleras of southern Peru and Bolivia appear to have expanded before the last global glacial maximum (Clapperton, 1993b). More frequent incursions of polar air masses from the southeast would bring cooler and cloudier conditions to the subtropical Andes throughout much of the year (Seltzer, 1990). Today more than 80% of the annual precipitation at the base of Sajama falls in the summer months (November–March). At this time solar radiation heats the Altiplano, facilitating the development of a low pressure centre in which the deep convection (over the warm Altiplano) facilitates the advection of moist air from the east (Vuille *et al.*, 1998).

The similarity of the  $\delta^{18}\text{O}$  values from Huascarán (Peru) and Sajama (Table 1) in both the Holocene and LGS suggests that the tropical Atlantic Ocean has remained the dominant moisture source for the tropical Andes. The drier conditions on Huascarán (9°S) and wetter conditions on Sajama (18°S) are consistent with LGS lake-level reconstructions (Street-Perrott and Harrison, 1984), when only 25% of the tropical lakes that have been studied were as high as today. In the Northern Hemisphere between 25° and 35°N, most of the lakes were higher than today (Benson, 1981, 1991; Broecker *et al.*, 1998; Street and Grove, 1976, 1979). Model experiments (Rind, 1998) suggest that this difference in lake levels is consistent with a reduction in the tropical latitudinal temperature gradient and in Hadley Cell intensity. The latter requires that the tropical Atlantic was cooler by ca. 5°C at the LGM (Webb *et al.*, 1997), a greater cooling than in the CLIMAP (1976, 1981) simulation. A reduced temperature gradient at low to subtropical latitudes weakens the Hadley circulation regardless of the mean temperature, which plays a secondary role (D. Rind, personal communication). The enhanced moisture content of LGM and DCR air masses and prolonged cloud cover in the subtropics would contribute to significant increases in accumulation, reduced evaporation and hence glacier expansion.

## Nature of the seasonal $\delta^{18}\text{O}$ –temperature relationship in the tropics

The ice-core  $\delta^{18}\text{O}$  records shown in Fig. 5 confirm that, like polar ice-cores, Andean ice-cores also record century-to-millennial scale temperature fluctuations. Table 1 illustrates that the cooler conditions of the LGS and the warmer Holocene are evident in ice-core records from pole to pole. In addition, the  $\delta^{18}\text{O}$  histories from the two Northern Hemisphere and two Andean ice-cores reveal the rapid warming at the end of the LGS and the return to cooler conditions (e.g. the YD or DCR) before the final warming to full Holocene conditions.

Recent, well-documented climate fluctuations of shorter

temporal duration are also preserved, particularly in the two Peruvian ice-cores. Quelccaya and Huascarán both record the most recent neoglaciation (e.g., Little Ice Age) more prominently than the polar cores (Figure 5). Quelccaya's annually dated 1500-yr  $\delta^{18}\text{O}$  record confirmed the Little Ice Age cooling in the tropics (Thompson *et al.*, 1986) as well as the twentieth century warming (Thompson *et al.*, 1993). Thus, on time-scales of decades to millennia, the  $\delta^{18}\text{O}$  histories preserved in tropical ice-cores appear to record large-scale atmospheric temperature changes.

The conundrum is that the seasonal relationship between temperature and  $\delta^{18}\text{O}$  in the tropics is opposite that found in the polar regions, where the most negative  $\delta^{18}\text{O}$  values characterise winter snowfall. Further, the seasonal temperature range in the tropics is only a few degrees, whereas the seasonal differences in the  $\delta^{18}\text{O}$  of Andean snowfall are much larger, often up to 20‰. These observations raise the question: If the most isotopically depleted (negative)  $\delta^{18}\text{O}$  values characterise summer precipitation in the tropics, how does  $\delta^{18}\text{O}$  in tropical precipitation record temperature over longer time scales?

Dansgaard (1964) and Dansgaard *et al.* (1973) used a Rayleigh fractionation model to satisfactorily explain the primary features of the global distribution of stable isotopes in precipitation and its relationship to both local temperatures and precipitation amount. The Rayleigh model assumes that the condensate forms in equilibrium with the surrounding vapour and is immediately removed from the air parcel. Obviously this is a simplification of the real atmospheric processes. Subsequently, Merlivat and Jouzel (1979) and Jouzel and Merlivat (1984) used a Rayleigh-based model to explore the relationship between the initial isotopic concentrations of the vapour as a function of sea-surface temperature (SST) and to account for kinetic fractionation associated with snow formation and evaporation. Use of  $\delta^{18}\text{O}$  and/or  $\delta\text{D}$  as palaeothermometers requires knowledge of the spatial isotope relationship and surface temperatures ( $T_s$ ) expressed as

$$\delta = aT_s + b \quad (1)$$

which is defined over a certain region and assumed to remain constant over time. (We have chosen to designate the coefficients as  $a$  and  $b$  rather than the usual  $\alpha$  and  $\beta$  to avoid confusion with the isotope fractionation factor.) Year-round observations at the South Pole by Aldaz and Deutsch (1967) confirmed the strong relationship between  $\delta^{18}\text{O}$  and atmospheric temperature above the surface inversion. Such early studies relating surface temperatures to the isotopic ratio in snowfall over the polar regions lead Dansgaard (1964) and Johnsen *et al.* (1989) to suggest a slope ( $a$ ) of 0.67‰ per °C for the spatial isotope relationship. More recently, the nature of the  $\delta$ - $T_s$  transfer function has come under some scrutiny (Cuffey *et al.*, 1995), particularly under different climatic regimes of the past. For example, recent calibrations using borehole temperatures demonstrate that isotopic ratios are a very good palaeothermometer over various time intervals but that the calibration (slope of the  $\delta$ - $T_s$  relationship) is different for the last few millennia. They demonstrated that the GISP2 and GRIP cores give values for  $a$  of 0.5‰°C<sup>-1</sup> to 0.6‰°C<sup>-1</sup>, respectively for the last few centuries, but values for  $a$  of ca. 0.33‰°C<sup>-1</sup> and 0.23‰°C<sup>-1</sup> for older ice (Cuffey *et al.*, 1995; Johnsen *et al.*, 1995; Jouzel *et al.*, 1997). Thus, even in the polar regions, application of the  $\delta$ - $T_s$  relationship remains under investigation. Likewise, application of isotopic thermometry in the tropics is ripe for further study.

Tropical South America is one of the warmest and wettest regions of the Earth, capable of supporting both the largest rain forest and greatest river discharge in the world. Positioned between 5°N and 15°S, the Amazonia region of Brazil (and parts of neighbouring countries) experiences a distinct wet–dry seasonal cycle that exceeds any minor seasonality in air temperature. The meridional migration of the Intertropical Convergence Zone (ITCZ) controls this seasonality and is amplified in the Amazonia region by the deep low pressure centre that develops owing to intense surface heating over the Bolivian Altiplano in the austral summer and autumn (January–May) (Virji, 1981).

For the Quelccaya ice-cap Grootes *et al.*, (1989) attempted to reconcile the large seasonal differences in  $\delta^{18}\text{O}$  and small seasonal temperature range by calculating a balance for water vapour mass and  $\delta^{18}\text{O}$ . As with previous studies, to make the problem tractable they treated the change of the  $\delta^{18}\text{O}$  of atmospheric water vapour as a Rayleigh process. The ratio of the current ( $R$ ) and original ( $R_0$ ) isotopic abundance ( $\delta^{18}\text{O}$ ) is given by the Rayleigh equation

$$R/R_0 = f^{(\alpha-1)} \quad (2)$$

where  $f$  is the fraction of the original amount of water vapour remaining in the air and  $\alpha$  is the isotopic fractionation factor at equilibrium (for liquid–vapour or ice–vapour). Thus the isotopic ratio of the precipitation ( $R_p$ ) is calculated from that of the vapour using the fractionation factor so that  $R_p = \alpha R_v$ . They converted these formulae to their relative deviation  $\delta$  from the V-SMOW standard as

$$\delta_v = f^{(\alpha-1)} (1000 + \delta_{v0}) - 1000 \quad \text{and} \quad \delta_p = \alpha(1000 + \delta_v) - 1000 \quad (3)$$

where subscripts v and p indicate vapour and precipitation and vo refers to the original vapour. Furthermore,  $\delta_{v0}$  can be determined from the conditions at the moisture source (i.e. sea surface) by the following expression

$$\delta_{v0} = (1000 + \delta_{sw})/\alpha - 1000 + \text{KE} \quad (4)$$

where KE is the kinetic effect (usually estimated at  $-3\text{‰}$ ) and  $\delta_{sw}$  is the isotopic composition of the source (seawater), approximately  $+1\text{‰}$  in the tropical ocean. The role of temperature in Rayleigh fractionation is actually twofold: it involves both the molecular physics of the phase changes of water (the temperature dependence of  $\alpha$ ,  $\ln \alpha = 1137 T^{-2} - 0.4156 T^{-1} - 0.0020667$  as determined by Majoube (1971)) as well as the larger indirect effects of the temperature dependence on saturation humidity (the Clausius–Clapeyron Equation).

Field observations and airflow patterns over tropical South America confirm that the tropical Atlantic Ocean to the east is the primary moisture source throughout the year (Taljaard, 1972). Thus, the Grootes *et al.*, (1989) model includes three steps, each using the Rayleigh process, as the water vapour moves from its source region over the tropical Atlantic to the Quelccaya ice-cap in the southern Andes of Peru. These stages are presented schematically in Fig. 6. The relationships expressed by equation 3 require that the isotopic composition of precipitation at the collection/deposition site ( $\delta_p$ ) will become more depleted as water vapour is removed (via precipitation/runoff) from the air mass as it continues across the land surface. Depletion occurs because the condensate is always more enriched than the remaining vapour, and by continuity, removal of this liquid from the isolated parcel requires the surrounding vapour to be increasingly more  $^{18}\text{O}$ -depleted. This process essentially describes the control of the water vapour budget (and hence, the hydrology of the region in question) on the isotopic composition of the

precipitation and, therefore, the effects of temperature on Rayleigh fractionation in nature are not immediately obvious.

Moisture advected from the Atlantic must traverse the Amazon Basin, where net water vapour removal varies from 0% in the dry season to 85% in the wet season. The result is a seasonal  $\delta^{18}\text{O}$  change of up to 18.4‰ in the precipitation falling at the base of the Andes on the western margin of the basin. Next, the air mass must ascend the eastern slopes of the Andes, a 5.6 km increase in surface elevation to reach Quelccaya. Adiabatic cooling and precipitation were considered under maximum wet and dry season conditions and the decrease in  $\delta^{18}\text{O}$  of the resulting precipitation was nearly identical for both scenarios (11.2 and 11‰, respectively). The summer snowfall over Quelccaya results from convective showers that can decrease the  $\delta^{18}\text{O}$  value by an additional 5‰, creating an expected seasonal range of  $\delta^{18}\text{O}$  in Quelccaya snowfall of  $-10.4$  to  $-33.7\text{‰}$ . However, post-depositional modification may enrich dry season snow that is subsequently retrieved from ice cores or pits. An enrichment of 6.3‰ was observed during the 1983 field season. The final result was a predicted  $\delta^{18}\text{O}$  range of  $-4.1$  to  $-33.7\text{‰}$  that compared very favourably with the range of ca.  $-8.0$  to  $-30.8\text{‰}$  from snow-pit samples (Fig. 6).

A different approach is now presented that further supports the idea that the physics of Rayleigh processes should not necessarily be abandoned in the pursuit of long-term stable isotope–temperature relationships in the tropics. In high-latitude regions, the consistent relationship between  $\delta^{18}\text{O}$  and  $T_s$  demands that condensation generally take place at a fixed height throughout the year. For the tropics, a seasonally changing mean condensation level (MCL) in the atmosphere could mean that temperature and humidity conditions are vastly different for dry season precipitation versus wet season precipitation. Hence, this strategy points to the cycle in deep convection over much of South America to explain the unusual  $\delta^{18}\text{O}$ – $T_s$  slope, seen also in most other low-latitude sites (Rozanski *et al.*, 1993).

As mentioned above, the process of Rayleigh fractionation, although limited, is a useful method for investigating the relationship between atmospheric conditions and stable isotope measurements. Using the formulae (equations 3 and 4) in reverse, a single elevation may be determined at which the atmospheric conditions (temperature, pressure and humidity) would generate the required  $f$  value for any given set of  $\delta_{v0}$  and  $\delta_p$  values. These seasonally varying conditions represent a theoretical equilibrium state for condensate falling through the changing air column; however, they could also represent a variable MCL in the mid-troposphere. As both these phenomena are associated with the same seasonal cycle in convective activity, it would be very difficult to parameterise them individually and thus, no distinction was attempted.

The data used in this analysis were available sea-surface temperatures (SSTs) in the tropical Atlantic (the average SSTs used were averaged from two grid points (1°N, 47°W and 7°S, 33°W), which yielded values in the range of ca. 27–28°C—these data were obtained from the ds277.0 ‘recon’ data set available by ftp from NCAR at <http://www.scd.ucar.edu/dss/datasets/ds277.0.html>) and the observed set of monthly  $\delta^{18}\text{O}$  values for inland sites such as Manaus (Fig. 7a and c) in the interior of Amazonia (3°S, 60°W). Between 1965 and 1987, 183 monthly averaged  $\delta^{18}\text{O}$  values were reported at Manaus as part of the International Atomic Energy Agency (IAEA) Global Network of Isotopes in Precipitation (GNIP) (Rozanski *et al.*, 1993). In addition, monthly averaged surface and upper air data are also available for Manaus from the journal *Monthly Climatic*

Data for the World (MCDW), for a similar time interval. These data include temperature, wind vectors, dew point and geopotential height for each of the standard levels of the lower and mid-troposphere (surface and 850, 700 and 500 hPa). Although discontinuous, the Manaus data are fairly consistently reported from 1967 to 1987, the period of concurrent isotope measurements. It is important to note that traditional radiosonde measurements of middle tropospheric humidity have been challenged by satellite observations (Sun and Lindzen, 1993), indicating that relative humidity at 500 hPa may be overestimated by as much as 20%. Additionally, the recent  $\delta^{18}\text{O}$  record from the Huascarán ice-core was used in this analysis, as the subannual variations are particularly well preserved at this site. In this case, the raw data for the period 1961–1987 were composited into 12 monthly means (Fig. 7b) by a time-averaging procedure discussed in more detail by Henderson *et al.*, (1999). Temporal uncertainty (on a month-to-month basis) and the diffusion of  $^{18}\text{O}$  during the firnification process will combine to make these estimates of the seasonal MCL migration minimum values.

For each month, equations (3) and (4) were solved simultaneously to determine the necessary final  $f$  value for precipi-

tation at the deposition site (either Manaus and Huascarán), given initial mixing ratios based upon the corresponding MCDW surface relative humidities (ca. 85–92%) for Belém (location shown in Fig. 7a). The initial  $\delta_{\text{vo}}$  over the Atlantic was determined from the monthly averaged SSTs as described at the start of the previous paragraph and the  $\alpha$  fractionation factors based on these temperatures. Values of +1‰ and –3‰ were used for the  $\delta_{\text{sw}}$  and the kinetic effect during vaporisation, respectively. Figure 8 shows the water vapour pressure ( $e$ ) states of the lower to mid-troposphere over Manaus for four of the 12 months, each representing a different season. Polynomial expressions that provided a best fit to the long-term data (as shown in Fig. 8 for  $e$  only) were derived for all three parameters, including the vertical profiles of temperature and pressure that are not shown, as both were necessary for the determination of  $\alpha$  (during condensation) and the final saturation mixing ratio. Together, these expressions allow identification of the specific elevation where the hydrological budget requirements based on the empirical isotope data were satisfied. Table 2 provides the results of these calculations for both Manaus and Huascarán.

Because the Huascarán drill-site is at an elevation of more

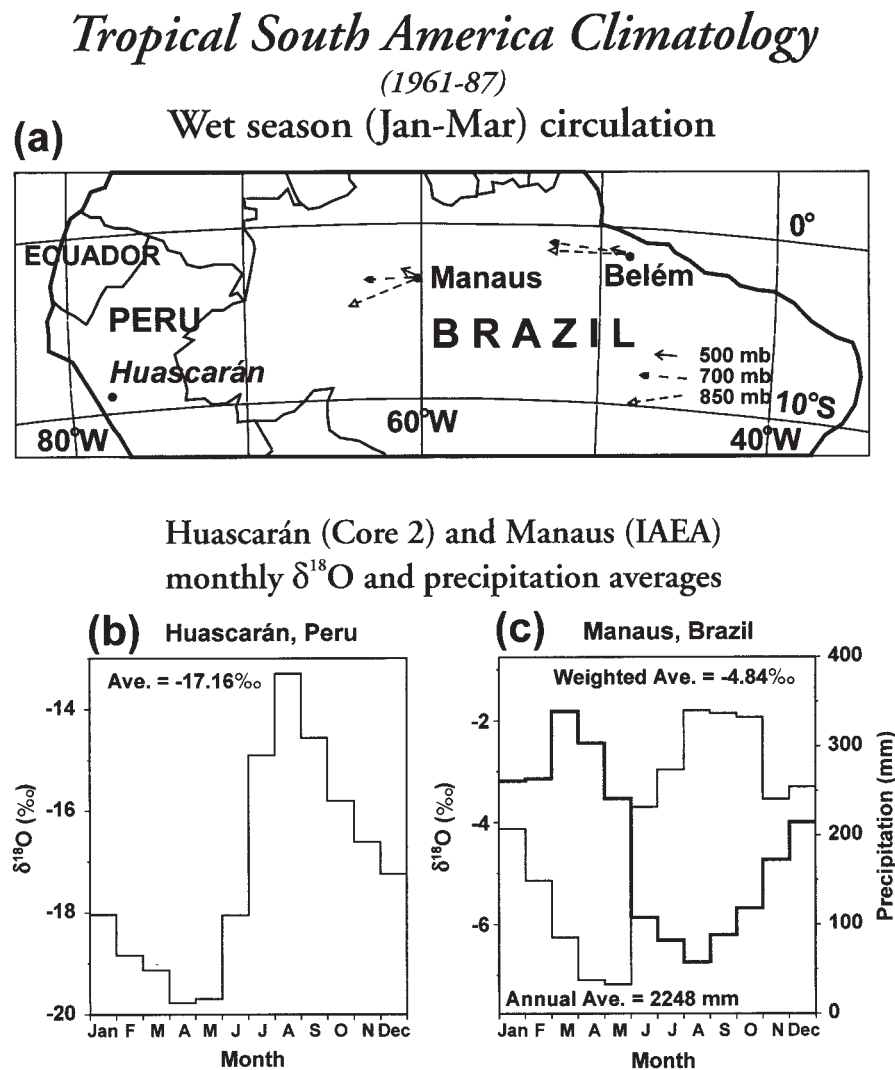


**Figure 7** (a) This map shows the location of Belém and Manaus in the Amazon Basin along with their mean summer (January through to March) wind directions at three atmospheric levels (850, 700 and 500 hPa). (b) Shown are the 12 monthly  $\delta^{18}\text{O}$  averages composited (Henderson *et al.*, 1999) from the Huascarán ice-core record from 1961 to 1987. (c) The monthly  $\delta^{18}\text{O}$  averages for Manaus are shown along with the monthly precipitation totals from 1967 to 1987. The annual average  $\delta^{18}\text{O}$  for Manaus is weighted to account for variations in monthly precipitation totals.

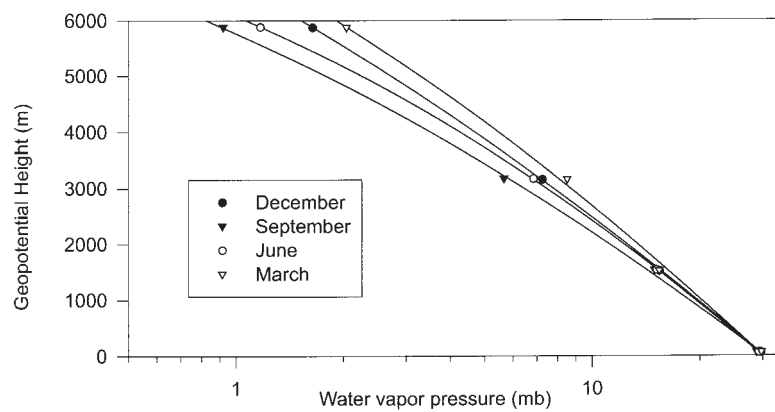


**Figure 8** Shown are four of the twelve monthly averages of water vapour pressure (mb) for Manaus, Brazil, calculated at the surface and at three atmospheric levels (850, 700 and 500 hPa). Solid lines represent the best-fit second order polynomial expressions used to determine the MCL consistent with monthly averaged  $\delta^{18}\text{O}$  values for Manaus and Huascarán.

**Table 2** Results from the simultaneous solution of equations (3) and (4) using monthly averaged  $\delta^{18}\text{O}$  values (1967–1987) to provide theoretical equilibrium atmospheric conditions for condensate formation at Huascarán and Manaus conditions. Range of elevations: 1933 m for Huascarán; 1950 m for Manaus

Month	Huascarán $\delta^{18}\text{O}$	MCL (m)	Temp. (°C)	Rel. Hum. (%)	Manaus $\delta^{18}\text{O}$	MCL (m)	Temp. (°C)	Rel. Hum. (%)
January	-18.04‰	4585	1.8	57.9	-4.12‰	460	23.5	85.6
February	-18.84‰	4615	1.2	57.5	-5.14‰	805	21.7	83.5
March	-19.13‰	4745	0.8	57.0	-6.26‰	1253	19.0	83.1
April	-19.77‰	4785	0.6	55.6	-7.10‰	1531	17.8	80.9
May	-19.69‰	4648	1.3	52.8	-7.18‰	1566	17.8	78.9
June	-18.05‰	4001	4.1	52.0	-3.70‰	249	25.2	83.2
July	-14.90‰	3258	7.6	56.7	-2.96‰	-27 <sup>a</sup>	27.1	80.7
August	-13.30‰	2852	10.1	57.3	-1.80‰	-384 <sup>a</sup>	30.3	78.7
September	-14.56‰	3142	8.9	52.5	-1.85‰	-196 <sup>a</sup>	29.2	80.7
October	-15.81‰	3581	6.8	50.1	-1.93‰	-65 <sup>a</sup>	28.3	80.8
November	-16.61‰	3968	4.8	52.0	-3.54‰	519	24.4	79.7
December	-17.24‰	4138	4.0	53.3	-3.30‰	246	25.6	82.5

<sup>a</sup>Surface conditions yield a  $\delta^{18}\text{O}$  value lower than observed (due to amount effect) and following extrapolation of the lapse rates, the back-calculation gives a condition that would exist only below ground. These four values are not used in the slope determination (Fig. 10).

than 6 km, the precipitation archived there actually lies at or above the expected corresponding MCL. It is difficult to estimate the effects of orographic uplift and local lapse rate variability on condensate formation and subsequent deposition on the ice cap, when compared with central Amazonia. However, because the assumption has been made previously that any further fractionation of condensate during vertical transport would occur according to the Rayleigh law, it does not matter whether the environment through which the condensate travels is progressively warmer and wetter, or colder and drier. For this reason, the vertical structure of the atmosphere over Manaus was used as a proxy for that in the region of the Andean front. Given the widespread uniformity of the Amazon climate regime from east-to-west, it is not likely the temperature or humidity profiles vary greatly between Manaus and the Andean front.

The results in Table 2 suggest that the seasonal oscillations in isotopic composition for tropical South America can be explained by a fluctuation in the MCL of about 2 km. Note that the variable MCLs suggested by the isotope data indicate roughly constant relative humidities for formation of precipitation at Huascarán and Manaus, ca. 55% and ca. 80%,

respectively. A quantitative error analysis of these findings seems unreasonable given the instrumental errors in the measurements, the uncertainties in the subannual time-scale of the ice core, and the indistinguishable nature of various processes during condensation/precipitation. Despite these simplifications, this result agrees well with our understanding of Hadley Cell behaviour.

Newell *et al.*, (1969) presented a diagram of the meridional profile of latent heat release in the troposphere as a function of height and latitude for the December–February season (Fig. 9a). Horel *et al.*, (1989) used outgoing longwave radiation (OLR) measurements from polar-orbiting satellites to track the N–S migration of the ITCZ and associated heating lows. Their results for a 7-yr observational period indicated that the centre of the OLR minimum migrated on average from 10°S, 55°W (central Amazonia) to 10°N, 83°W (Central America) each year (Fig. 9b). Using the latent heat release maximum as a proxy for the MCL, an annual 20° latitude shift of the Hadley cell over Central and South America would result in a 1.7 km range in the mean elevation for condensation (Fig. 9a). It is important to note that the 1.7 km elevation change is likely to be a minimum value, as

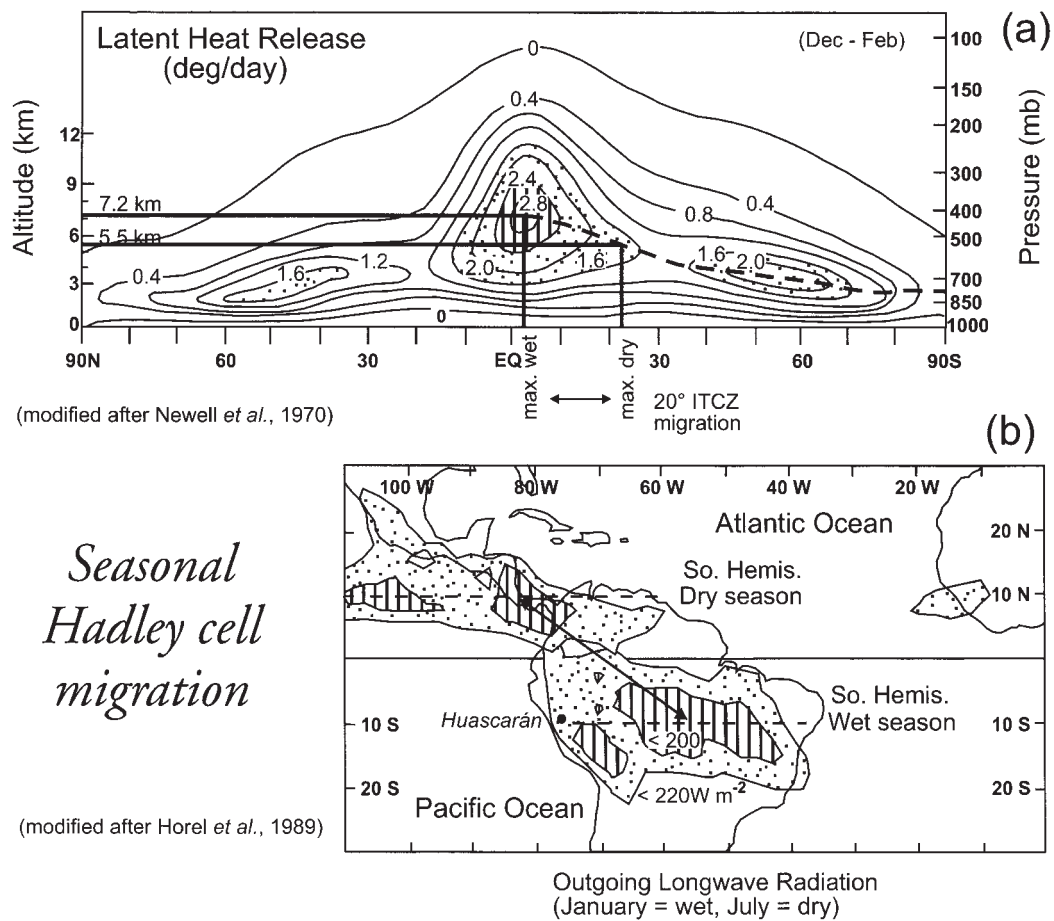


**Figure 9** (a) The meridional profile of latent heat (LH) release in the troposphere is shown for December–February (modified from Newell *et al.*, 1969). (b) The seasonal migration of the ITCZ and associated low-pressure regions was inferred from 7 yr of OLR measurements by Horel *et al.*, (1989). Coupled with (a) and assuming that the atmospheric region of maximum LH release (dashed line) approximates the MCL, a 20° latitude shift in the Hadley Cell would result in a seasonal change of 1.7 km in the height of the MCL.

Newell's profile is a 3-month zonal average and the range in convective heights between the wet and dry seasons would be at a maximum over Brazil. Of course, this simple graphical approach assumes that the shape of the latent heat contours within the Hadley Cell remains roughly constant from season to season, and that the  $>2.8^{\circ} \text{ day}^{-1}$  maximum just reaches the latitude of Huascarán ( $9^{\circ}\text{S}$ ). This assumption seems reasonable according to the Horel *et al.* (1989) analysis.

Because the latent heat argument and the isotopic results are in good agreement, and provide an additional mechanism for Rayleigh fractionation, we can now compare this scenario with the water budget explained in the Grootes *et al.*, (1989) model. As the initial and final mixing ratios that define  $f$  for the back-calculations do not strictly relate to the large-scale water budget (instead allowing  $f$  to be controlled by the changing/evolving vertical structure), it may appear that the two fractionation mechanisms might be additive, i.e. that  $^{18}\text{O}$  would be depleted both by the surplus of precipitation over evapotranspiration during the wet season, and also by the lifting of the wet season condensation level. However, it is likely that these two mechanisms are one and the same, such that the changes in the vertical profile of humidity are a direct result of the changes in the convergence-driven cumulative loss of moisture during westward mass transport. Low-level directional convergence of moisture over the Amazon lowlands drives vertical velocities in mesoscale towers that not only lead to tremendous rainout, but also are responsible for charging the middle troposphere with its mean humidity state (Sun and Lindzen,

1993), by evaporation of hydrometeors (lifted droplets and ice crystals) into the air surrounding the towers.

For demonstration purposes only, the MCL calculations have the advantage of providing estimates of air temperatures that serve as tropical analogues to the surface temperatures used to develop the high-latitude palaeothermometry equation, e.g. the values of  $a$  and  $b$  for equation (1). By plotting monthly  $\delta^{18}\text{O}$  against the variable height temperatures from Table 2 (Fig. 10), a relationship similar to that for high latitudes may be developed. Using Huascarán data alone, a slope of  $+0.63\text{‰}^{\circ}\text{C}^{-1}$  was produced from the variable height temperatures (circles), compared with a steep 'reverse' slope of  $-4.88\text{‰}^{\circ}\text{C}^{-1}$  when using the monthly 500 hPa temperatures over Manaus (squares) as a proxy for temperatures at the Huascarán col. Similarly, the Manaus data provide additional values (triangles and diamonds) that fall along a similar line, although with a more gradual slope ( $+0.49\text{‰}^{\circ}\text{C}^{-1}$ ). When combined, the points from both low elevation (triangles) and high elevation (circles) define a line similar to that in polar regions, with  $a = 0.67\text{‰}^{\circ}\text{C}^{-1}$  and  $b = -20.0\text{‰}$ . Furthermore, the lower value for the  $\delta^{18}\text{O}-T$  intercept might be expected for a tropical site given the warmer initial equilibrium temperature, as previously noted by Boyle (1997).

The preceding results are not intended to be interpreted as proof of a single global temperature– $\delta^{18}\text{O}$  relationship, but to illustrate the internal consistency of the arguments above. Even in high latitudes, the well-documented temperature dependence of  $\delta^{18}\text{O}$  is principally an indirect effect of

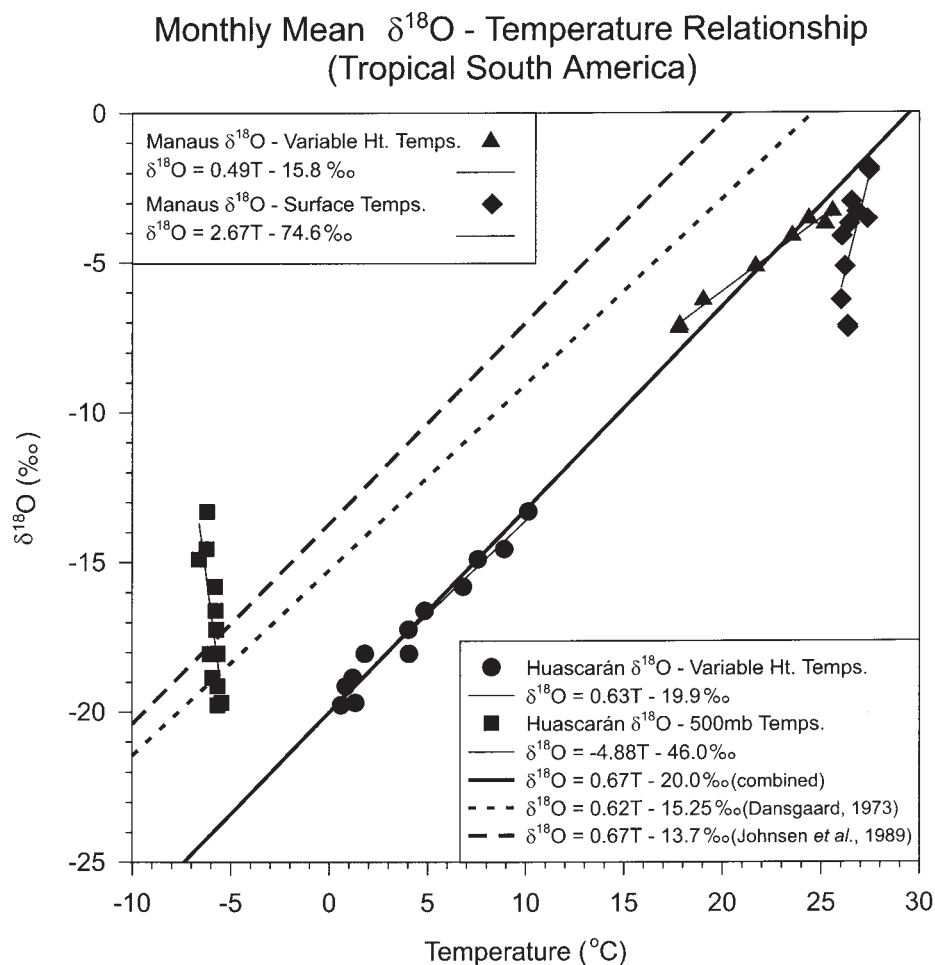


**Figure 10** The tropical  $\delta^{18}\text{O}$  -  $T$  relationships (derived from long-term monthly averages) based separately on surface air temperatures ( $T_s$ ) and variable height temperatures that relate to a seasonally evolving MCL, as described in text, are compared here. Shown for Huascarán are the 12 individual monthly solutions (Table 2), and the eight above-ground results from the Manaus analysis. In each case, the thin solid lines indicate a linear regression through the points shown (formulae given in the legends). Also shown (heavy extended line) is a linear regression through all 20 points from Huascarán and Manaus combined. Two separate high-latitude  $\delta^{18}\text{O}$ - $T_s$  expressions are included for comparison.

the control of temperature-dependent saturation humidity on the  $f$  value. So, rather than saying that past temperature relationships should be similar between low and high latitudes, the attempt here was to illustrate the effects of the different water budgets and to suggest that it is the dynamic (vertical) nature of the tropical atmosphere that drives the unusual  $\delta^{18}\text{O}$ - $T_s$  relationship for Amazon-Andean precipitation. Therefore, the physics of Rayleigh processes may still be applicable for understanding the long-term isotope-temperature relationships in the tropics, although quantitative methods are still uncertain at this stage. This deficiency is compounded by the apparent dissociation between modern and past  $\delta^{18}\text{O}$ - $T_s$  slopes ( $a$  values) for Greenland cores, supported both by borehole temperatures (Cuffey *et al.*, 1995) and gas isotopic methods (Severinghaus and Brook, 1999). Suspected effects on isotopic values by changing the seasonal distribution of snow accumulation may very well be important also for tropical sites, but this phenomenon remains undetectable at this time.

### Twentieth century warming and the fate of tropical ice-fields

The general warming of the twentieth century is now well documented. Although not all regions of the Earth have

warmed, the globally averaged temperature has increased  $0.7^\circ\text{C}$  since the end of the last century (Hansen *et al.*, 1999). Owing to the unpredictability of the natural climate system it is impossible to know with assurance whether this warming will continue unabated over the next few decades. The overwhelming scientific consensus (IPCC, 1996) suggests that without a natural forcing toward a cooler global climate regime, the current warming trend would be expected to continue in the coming decades. Warmer conditions are expected to bring both positive and negative impacts and these will be distributed unequally. One change that has been observed already is the rise in global sea-level (IPCC, 1996). This rise is due in part to the thermal expansion of the oceans and in part to the melting of smaller ice caps and glaciers, such as those discussed in the previous sections of this paper.

Evidence is accumulating for a strong warming in the tropics with the potential to drive the retreat and, in some cases, the disappearance of these smaller ice caps and glaciers at high elevations in the tropics and subtropics. Such ice masses are particularly sensitive to small changes in ambient temperatures as they already exist very close to the melting point. This warming and the concomitant retreat of the Quelccaya ice-cap (Peru) is now well documented (Brecher and Thompson, 1993; Thompson *et al.*, 1993). The  $\delta^{18}\text{O}$  records confirm both the atmospheric warming and physiological changes in the ice cap. Since 1976 Quelccaya

has been visited repeatedly for extensive monitoring and sampling. In addition to the deep drilling in 1983, shallow cores were taken from the summit of the ice cap in 1976 and 1991. Figure 11 compares the 1979, 1991 and 1995  $\delta^{18}\text{O}$  records from the summit along with the  $\delta^{18}\text{O}$  records from three additional cores taken in 1979 at successively lower elevations to the west. These records demonstrate that the seasonally resolved palaeoclimatic record, preserved as  $\delta^{18}\text{O}$  variations in 1979 and 1983 (Thompson *et al.*, 1986), is no longer retained within the currently accumulating snow. The percolation of meltwater throughout the accumulating snow pack has homogenised the stratigraphic record of  $\delta^{18}\text{O}$ . Note that the  $\delta^{18}\text{O}$  average for the 1991 summit core is 2‰ more enriched than for ice within the comparable depth interval in 1979. The  $\delta^{18}\text{O}$  records from three additional cores drilled in 1979 at successively lower elevations show clearly the isotopic smoothing by percolation of meltwater (Fig. 11). In 1979 Site 4 was clearly above the 0°C isotherm that is inferred to lie near Site 3 and well above Site 2. By 1991 the 0°C isotherm was certainly near

the summit of Quelccaya (Site 4), which implies that it had risen roughly 100 m in the intervening 12 yr. This increase in the height of the 0°C isotherm is clearly a sign of atmospheric warming in this region of the Andes.

The Quelccaya ice cap is also retreating (Brecher and Thompson, 1993). The Qori Kalis Glacier, a valley glacier on the western side of Quelccaya, has been monitored using terrestrial photogrammetry since 1978. The retreat of the ice front and the volume loss have been determined for six time intervals. These observations document a drastic retreat of the glacier that has accelerated with time. The latest photographic evidence from 1998 indicates that this retreat continues to accelerate. The retreat was twice as great in the latest 3-yr period, between 1995 and 1998, as it was in the previous 2-yr period, between 1993 and 1995 (48.7 versus 28.7 m yr<sup>-1</sup>). The rate of retreat is now an order of magnitude greater than it was between 1963 and 1978, when comparison between the position from the first terrestrial photography and the position from the aerial photographs gave a retreat rate of 4.9 m yr<sup>-1</sup>. The volume loss has accelerated

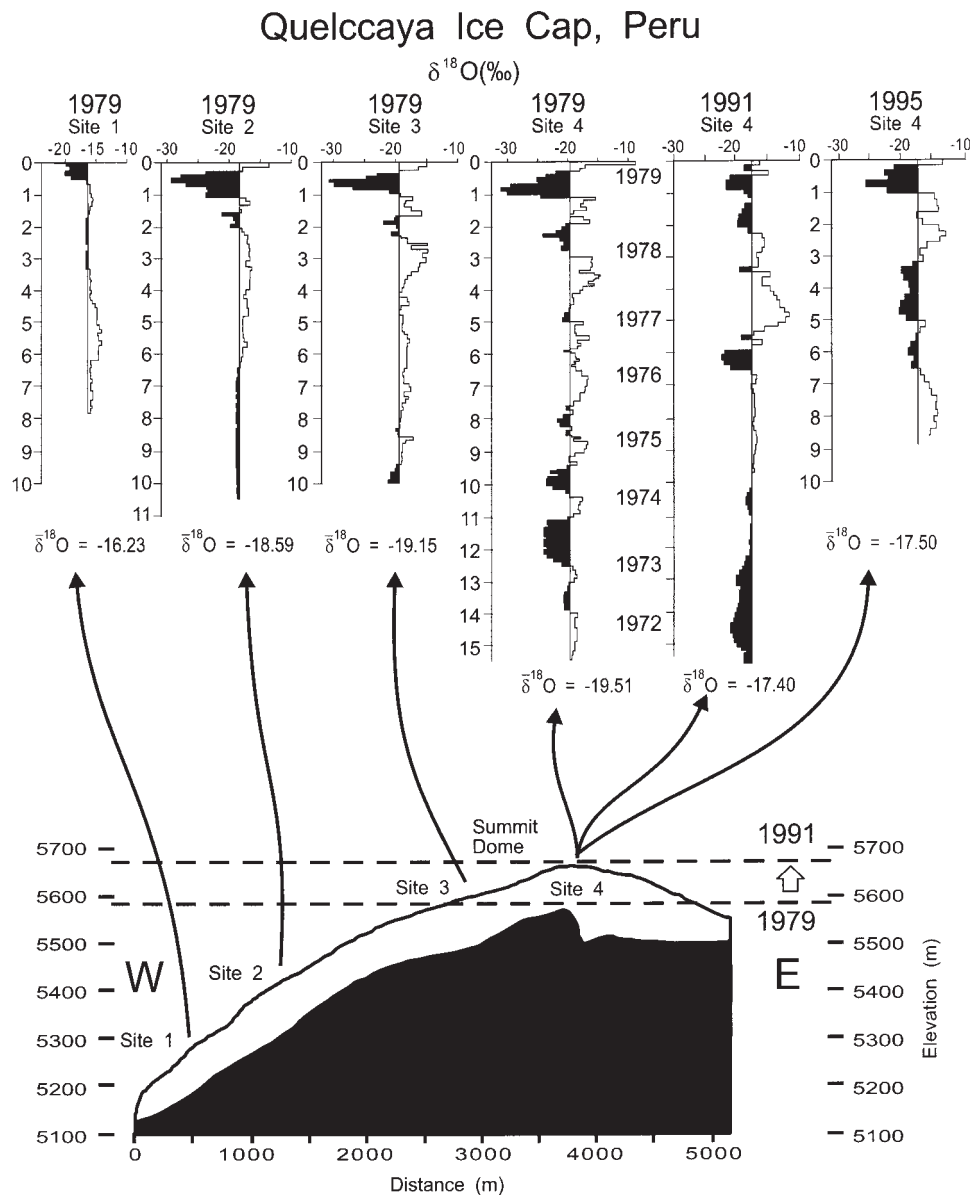


**Figure 11** The  $\delta^{18}\text{O}$  measurements from shallow cores collected on Quelccaya in 1979, 1991 and 1995 illustrate the smoothing of the  $\delta^{18}\text{O}$  record by meltwater percolation. The annual signal preserved at the summit (Site 4) in 1979 is not well preserved in the 1991 and 1995 cores from the same site. The isotopic smoothing at the summit site is comparable to that observed in cores drilled at lower elevation (Sites 1, 2 and 3). These observations indicate that the 0°C isotherm has risen roughly 100 m since 1979.

# Time Perspective of Climatic Change from Andes of Peru

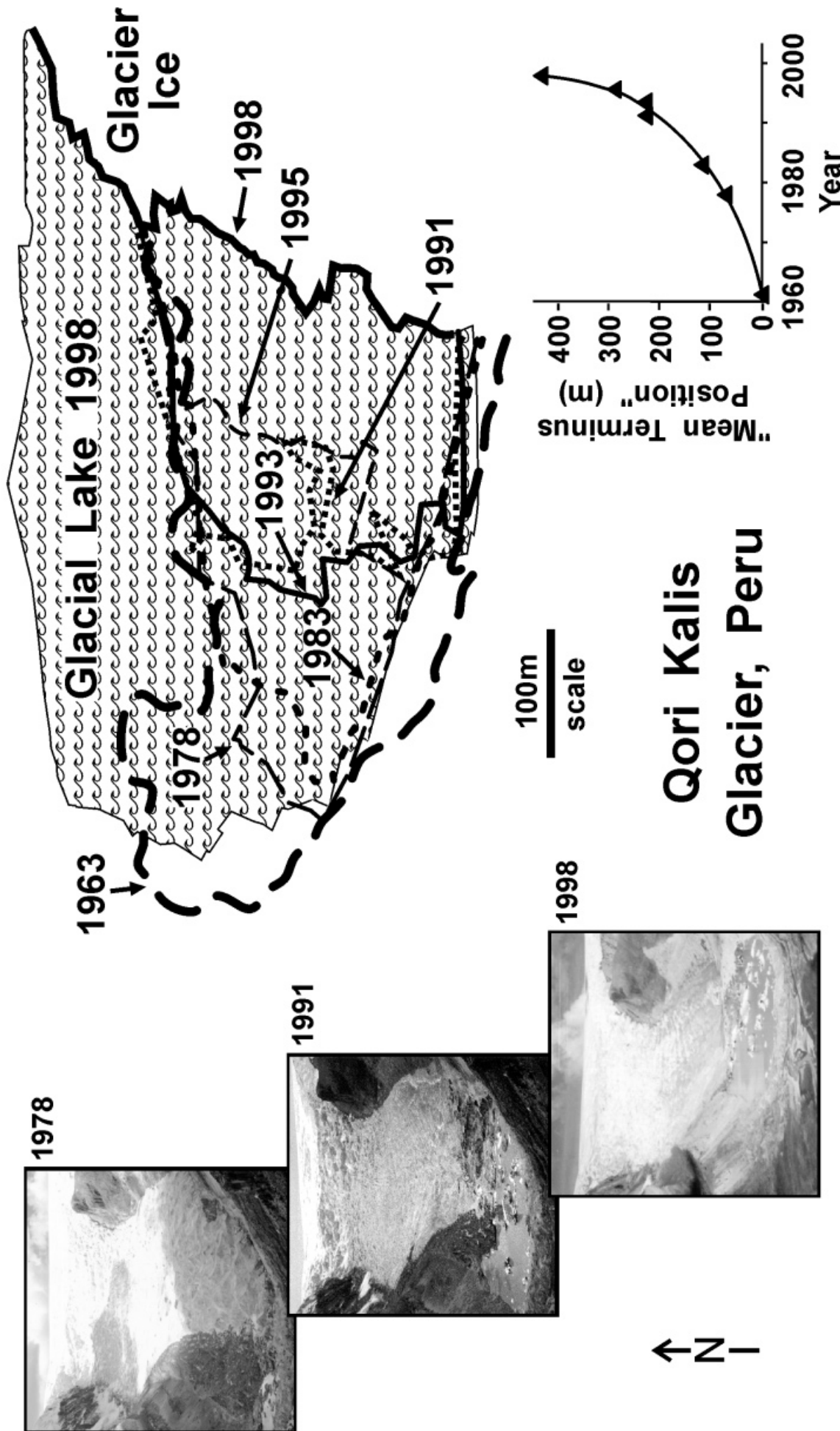


**Figure 12** The photographs (1978, 1991 and 1998) and the sketch map show the rapid retreat of the terminus of the Qori Kallis Glacier and the concomitant growth in the proglacial lake at the glacier toe. The graph (lower right) illustrates the accelerating rate of retreat since Qori Kallis was first mapped in 1963.

at an even greater rate. The graph in the lower right of Fig. 12 illustrates the retreat of the terminus. The sketch map shows the position of the glacier terminus for each of the seven determinations since 1963. Note that the small proglacial lake that first appeared in the 1991 photograph has continued to grow with the retreat of the ice front and in 1998 it was twice as large as in 1991 (Fig. 12).

Additional glaciological evidence for tropical warming exists. Hastenrath and Kruss (1992) report that the total ice cover on Mount Kenya had decreased by 40% between 1963 and 1987 and today it continues to diminish. The Speke glacier in the Ruwenzori Range of Uganda has retreated substantially since it was first observed in 1958 (Kaser and Noggler, 1991). Today the total ice mass on Kilimanjaro is roughly 25% of that which existed in 1912 (Hastenrath and Greischar, 1997). The shrinking of these ice masses in the high mountains of Africa and South America is consistent with similar observations throughout most of the world. It is important to note that this general retreat of high elevation tropical glaciers is concurrent with an increase in water-vapour content of the middle troposphere (Flohn *et al.*, 1990) in the tropics. Water vapour feedback effects may be partially responsible for the enhancement of warming at this level in the atmosphere of the tropics and subtropics (Diaz and Graham, 1996).

Finally, the tropical and subtropical ice-core records have the potential to provide annual to millennial-scale records of El Niño–Southern Oscillation events and monsoon variability and will provide further insight to the magnitude and frequency of these large-scale events. The earlier sections of this paper demonstrated that these ice cores preserve archives of decadal- to millennial-scale climatic and environmental variability. Further, they provide unique insights to both regional- and global-scale events ranging from the so-called ‘Little Ice Age’, the Younger Dryas (or DCR) cold phase, to the Late Glacial Stage. Despite their great palaeoclimatic potential these high-elevation ice fields are also quite vulnerable to increases in atmospheric temperature (Kaser *et al.*, 1996a). Recent glacier observations in tropical South America (Thompson *et al.*, 1993; Ames, 1996; Kaser *et al.*, 1996b) clearly demonstrate that many of these unique archives are in imminent danger of being lost if the current warming persists.

*Acknowledgments* We thank the many scientists, technicians, graduate students and field support personnel from The Ohio State University, OSTROM and the mountain guides of the Casa de Guías, Huaraz, Peru. In particular, we acknowledge the outstanding Ice Core Paleoclimate Research Group at Byrd Polar Research Center (Jihong Cole-Dai, Mary Davis, Ping-Nan Lin, Vladimir Mikhalenko and Victor Zagorodnov). A special thanks to drilling engineer Bruce Koci who worked on all of these projects. Jeannie Jaros assisted with the figures. This work has been supported over the years by the National Science Foundation ATM89–16635 and the National Oceanic and Atmospheric Administration NA16RC0525–01 and NA76GP0025. This is contribution number 1178 of the Byrd Polar Research Center.

## References

- Abbott MB, Binford MW, Brenner M, Kelts KR. 1997. A 3500 <sup>14</sup>C yr high-resolution record of water-level changes in Lake Titicaca, Bolivia/Peru. *Quaternary Research* **47**: 169–180.
- Aldaz L, Deutsch S. 1967. On a relationship between air temperature and oxygen isotope ratio of snow and firn in the South Pole region. *Earth and Planetary Science Letters* **3**: 267–274.
- Alley RB, Shuman CA, Meese DA, Gow AJ, Taylor KC, Cuffey KM, Fitzpatrick JJ, Grootes PM, Zielinski GA, Ram M, Spinelli G, Elder B. 1997. Visual-stratigraphic dating of the GISP2 ice core: basis, reproducibility, and application. *Journal of Geophysical Research* **102**: 26 367–26 381.
- Ames A. 1998. A documentation of glacier tongue variations and lake development in the Cordillera Blanca, Peru. *Zeitschrift für Gletscherkunde und Glazialgeologie* **34**: 1–36.
- Bard E. 1998. Geochemical and geophysical implications of the radiocarbon calibration. *Geochimica et Cosmochimica Acta* **62**: 2025–2038.
- Bard E, Arnold M, Maurice P, Duprat J, Moyes J, Duplessy J-C. 1987. Retreat velocity of the North Atlantic polar front during the last deglaciation determined by <sup>14</sup>C accelerator mass spectrometry. *Nature* **328**: 791–794.
- Bard E, Rostek F, Sonzogni C. 1997. Interhemispheric synchrony of the last deglaciation inferred from alkenone palaeothermometry. *Nature* **385**: 707–710.
- Beck JW, Récy J, Taylor F, Edwards RL, Cabioch, G. 1997. Abrupt changes in early Holocene tropical sea surface temperature derived from coral records. *Nature* **385**: 705–707.
- Benson LV. 1981. Paleoclimatic significance of lake-level fluctuations in the Lake Lahontan Basin. *Quaternary Research* **16**: 390–403.
- Benson LV. 1991. Timing of the last high-stand of Lake Lahontan. *Journal of Paleolimnology* **5**, 115–126.
- Boyle EA. 1997. Cool tropical temperatures shift the global  $\delta^{18}\text{O}-T$  relationship: an explanation for the ice core  $\delta^{18}\text{O}$  – borehole thermometry conflict? *Geophysical Research Letters* **24**: 273–276.
- Brecher HH, Thompson LG. 1993. Measurement of the retreat of Qori Kalis in the tropical Andes of Peru by terrestrial photogrammetry. *Photogrammetric Engineering and Remote Sensing* **59**: 1017–1022.
- Broecker WS, Denton GH. 1990. Implications of global snowline lowering during glacial time to glacial theory. *Quaternary Science Reviews* **9**: 305–341.
- Broecker WS, Peteet D, Hajdas I, Lin J, Clark E. 1998. Antiphasing between rainfall in Africa’s Rift Valley and North America’s Great Basin. *Quaternary Research* **50**: 12–20.
- Bush MB, Colinvaux PA, Weimann MC, Piperno DR, Liu K. 1990. Late Pleistocene temperature depression and vegetation change in Ecuadorian Amazonia. *Quaternary Research* **34**: 330–345.
- Clapperton CM. 1993a. *Quaternary Geology and Geomorphology of South America*. Elsevier Science Publishers: Amsterdam.
- Clapperton CM. 1993b. Nature of environmental changes in South America at the Last Glacial Maximum. *Palaeogeography, Palaeoclimatology, Palaeoecology* **101**: 189–208.
- Clapperton CM. 1993c. Glacier readvances in the Andes at 12500–10000 yr BP: implications for mechanism of late-glacial climatic change. *Journal of Quaternary Science* **8**: 197–215.
- Clapperton CM, Clayton JD, Benn DI, Marden, CJ, Argollo J. 1997. Late Quaternary glacier advances and palaeolake high stands in the Bolivian Altiplano. *Quaternary International* **38/39**: 49–59.
- CLIMAP Project Members. 1976. The surface of the ice-age earth. *Science* **191**: 1131–1137.
- CLIMAP Project Members. 1981. Seasonal reconstruction of the Earth’s surface at the last glacial maximum. *Geological Society of America, Chart and Map Series* **36**.
- Colinvaux PA, De Oliveira PE, Moreno JE, Miller MC, Bush MB. 1996. A long pollen record from lowland Amazonia; forest and cooling in glacial times. *Science* **274**: 85–88.
- Cuffey KM, Clow GD, Alley RB, Stuvier M, Waddington ED, Saltus RW. 1995. Large Arctic temperature change at the Wisconsin–Holocene glacial transition. *Science* **270**: 455–458.
- Damuth, JE, Fairbridge, RW. 1970. Equatorial Atlantic deep-sea arkosic sands and ice-age aridity in tropical South America. *Geological Society of America Bulletin* **81**: 189–206.
- Dansgaard W. 1964. Stable isotopes in precipitation. *Tellus* **16**: 436–468.
- Dansgaard W, Oeschger H. 1989. Past environmental long-term records from the Arctic. In *The Environmental Record in Glaciers and Ice Sheets*, Oeschger H, Langway CC Jr (eds). Wiley: Chichester, 287–317.

- Dansgaard W, Johnsen S, Clausen HB, Gundestrup N. 1973. Stable isotope glaciology. *Meddelelser Om Grønland* **192**: 1–53.
- Diaz HF, Graham NE. 1996. Recent changes in tropical freezing heights and the role of sea surface temperature. *Nature* **383**: 152–155.
- Flohn H, Kapala A, Knoche HR, Machel H. 1990. Recent changes of the tropical water energy budget and of mid-latitude circulations. *Climate Dynamics* **4**: 237–252.
- Grootes PM, Stuiver M, Thompson LG, Mosley-Thompson E. 1989. Oxygen isotope changes in tropical ice, Quelccaya, Peru. *Journal of Geophysical Research* **94**: 1187–1194.
- Grootes PM, Stuiver M, White JWC, Johnsen S, Jouzel J. 1993. Comparison of oxygen isotope records from the GISP2 and GRIP Greenland ice cores. *Nature* **366**: 552–554.
- Guilderson TP, Fairbanks RG, Rubenstein JL. 1994. Tropical temperature variations since 20,000 years ago; modulating interhemispheric climate change. *Science* **263**: 663–665.
- Haberle SG, Maslin MA. 1999. Late Quaternary vegetation and climate change in the Amazon Basin based on a 50,000 year pollen record from the Amazon Fan, ODP Site 932. *Quaternary Research* **51**: 27–38.
- Hammer CU, Clausen HB, Dansgaard W, Neftel A, Kristinsdottir P, Johnsen E. 1985. Continuous impurity analysis along the Dye 3 deep core. In *Greenland Ice Core* Langway Jr. CC, Oeschger H, Dansgaard H (eds). American Geophysical Union: Washington, DC: 90–94.
- Hansen J, Ruedy R, Glascoe J, Sato M. 1999. GISS analysis of surface temperature change. *Journal of Geophysical Research* **104**: 30 997–31 022.
- Hastenrath S, Greischar L. 1997. Glacier recession on Kilimanjaro, East Africa, 1912–1989. *Journal of Glaciology* **43**: 455–459.
- Hastenrath S, Kruss PD. 1992. The dramatic retreat of Mount Kenya's glaciers between 1963 and 1987. Greenhouse forcing. *Annals of Glaciology* **16**: 127–133.
- Hastenrath S, Kutzbach J. 1985. Late Pleistocene climate and water budget of the South American Altiplano. *Quaternary Research* **24**: 249–256.
- Henderson KA, Thompson LG, Lin P-N. 1999. The recording of El Niño in ice core  $\delta^{18}\text{O}$  records from Nevado Huascarán, Peru. *Journal of Geophysical Research* **104**: 31 053–31 066.
- Herd DG, Naeser CW. 1974. Mountain snowline lowering in the tropical Andes. *Geology* **2**: 603–604.
- Horel JD, Hahmann AN, Geisler JE. 1989. An investigation of the annual cycle of convective activity over the tropical Americas. *Journal of Climate* **2**: 1388–1403.
- Intergovernmental Panel on Climate Change. 1996. *Climate Change 1995*. Houghton JT, Meira Filho LG, Callandar BA, Harris N, Kattenberg A, Maskell K (eds). Cambridge University Press: Cambridge.
- Johnsen SJ, Dansgaard W, Clausen HB, Langway Jr CC. 1972. Oxygen isotope profiles through the Antarctic and Greenland ice sheets. *Nature* **235**: 429–434.
- Johnsen S, Dansgaard W, White JW. 1989. The origin of Arctic precipitation under present and glacial conditions. *Tellus* **41**: 452–469.
- Johnsen S, Dahl-Jensen D, Dansgaard W, Gundestrup NS. 1995. Greenland temperatures derived from GRIP bore hole temperature and ice core isotope profiles. *Tellus* **B47**: 624–629.
- Jouzel J, Merlivat L. 1984. Deuterium and oxygen 18 in precipitation: modeling of the isotopic effects during snow formation. *Journal of Geophysical Research* **89**: 11 749–11 757.
- Jouzel J, Lorius C, Petit JR, Genthon C, Barkov NI, Kotlyakov VM, Petrov VM. 1987. Vostok ice core: a continuous isotope temperature record over the last climatic cycle (160,000 years). *Nature* **329**: 403–408.
- Jouzel J, Alley RB, Cuffey CM, Dansgaard W, Grootes P, Hoffman G, Johnsen SJ, Koster RD, Peel D, Shuman CA, Stievenard M, Stuiver M, White J. 1997. Validity of the temperature reconstruction from water isotopes in ice cores. *Journal of Geophysical Research* **102**: 26 471–26 487.
- Kaser G, Noggler B. 1991. Observations on Speke Glacier, Ruwenzori Range Uganda. *Journal of Glaciology* **37**: 315–318.
- Kaser G, Hastenrath S, Ames A. 1996a. Mass balance profiles on tropical glaciers. *Zeitschrift für Gletscherkunde und Glazialgeologie* **32**: 75–81.
- Kaser G, Georges Ch, Ames A. 1996b. Modern glacier fluctuations in the Huascarán–Chopicalqui Massif of the Cordillera Blanca, Peru. *Zeitschrift für Gletscherkunde und Glazialgeologie* **32**: 91–99.
- Kessler A. 1985. Reconstruction of Late Glacial climate and water balance on the Peruvian–Bolivian Altiplano. *Zeitschrift für Gletscherkunde und Glazialgeologie* **21**: 107–114.
- Klein AG, Isacks BL, Bloom AL. 1995. Modern and Last Glacial Maximum snowline in Peru and Bolivia: implications for regional climatic change. *Bulletin de l'Institut Français d'Études Andines* **24**: 607–617.
- Majoube M. 1971. Fractionnement en oxygène 18 et en deutérium entre l'eau et sa vapeur. *Journal de Chimie Physique et de Physico-chimie Biologique* **68**: 1423–1436.
- Mercer JH. 1969. The Allerød Oscillation: a European climatic anomaly? *Arctic and Alpine Research* **1**: 227–234.
- Mercer JH. 1984. Late Cainozoic glacier variations in South America south of the equator. In *Late Cainozoic Palaeoclimates of the Southern Hemisphere*, Vogel JC (ed.). Balkema: Rotterdam: 45–58.
- Merlivat L, Jouzel J. 1979. Global climatic interpretation of the deuterium-oxygen 18 relationship for precipitation. *Journal of Geophysical Research* **84**: 5029–5033.
- Minchin J. 1882. Notes on a journey through part of the Andean tableland of Bolivia. *Proceedings of the Royal Geographical Society* **4**: 67.
- Mosley-Thompson E, Thompson LG. 1994. Dust in polar ice sheets. *Analisis* **22**: 44–46.
- Newell RE, Vincent DG, Dopplick TG, Ferruzza D, Kidson JW. 1970. The energy balance of the atmosphere. In *The Global Circulation of the Atmosphere* Corby GA (ed.). Royal Meteorological Society: London: 42–90.
- Peteet D. 1995. Global Younger Dryas? *Quaternary International* **28**: 93–104.
- Petit JR, Briat M, Royer M. 1981. Ice age aerosol content from East Antarctic ice core samples and past wind strength. *Nature* **293**: 391–394.
- Porter SC. 1979. Glacial snowline lowering in Hawaii. *Geological Society of America Bulletin* **90**: 980–1093.
- Rind D. 1998. Latitudinal temperature gradients and climate change. *Journal of Geophysical Research* **103**: 5943–5971.
- Rind D, Peteet D. 1985. Terrestrial conditions at the last glacial maximum and CLIMAP sea-surface temperature estimates: are they consistent? *Quaternary Research* **24**: 1–22.
- Robertson GP, Tiedje JM. 1988. Deforestation alters denitrification in a lowland tropical rain forest. *Nature* **336**: 756–759.
- Rodbell DT. 1992. Snowline lowering in the Peruvian Andes. *Boreas* **21**: 43–52.
- Rozanski K, Araguás-Araguás L, Gonfiantini R. 1993. Isotopic patterns in modern global precipitation. In *Climate Change in Continental Isotopic Records*, Swart PK, Lohmann KC, McKenzie J, Savin J (eds). American Geophysical Union: Washington, DC: 1–36.
- Schrag DP, Hampt G, Murray DW. 1996. Pore fluid constraints on the temperature and oxygen isotopic composition of the glacial ocean. *Science* **272**: 1930–1932.
- Seltzer GO. 1990. Recent glacial history and paleoclimate of the Peruvian–Bolivian Andes. *Quaternary Science Reviews* **9**: 137–152.
- Seltzer GO. 1992. Late Quaternary glaciation of the Cordillera Real, Bolivia. *Journal of Quaternary Research* **7**: 87–98.
- Seltzer GO. 1994. A lacustrine record of late Pleistocene climatic change in the subtropical Andes. *Boreas* **23**: 105–111.
- Severinghaus JP, Brook EJ. 1999. Abrupt climate change at the end of the Last Glacial Period inferred from trapped air in polar ice. *Science* **286**: 930–934.
- Steig EJ, Brook EJ, White JWC, Sucher CM, Bender ML, Lehman SJ, Morse DL, Waddington ED, Clow GD. 1998. Synchronous climate changes in Antarctica and the North Atlantic. *Science* **282**: 92–95.
- Street FA, Grove AT. 1976. Environmental and climatic implications of late Quaternary lake-level fluctuations in Africa. *Nature* **261**: 385–389.

- Street FA, Grove AT. 1979. Global maps of lake-level fluctuations since 30,000 yr B.P. *Quaternary Research* **12**: 83–118.
- Street-Perrott FA, Harrison SA. 1984. Temporal variations in lake levels since 30,000 yr BP—an index of the global hydrological cycle. In *Climate Processes and Climate Sensitivity*, Hansen JE, Takahashi T (eds). American Geophysical Union: Washington, DC.
- Stuiver M, Reimer PJ. 1993. Calibration review 3. *Radiocarbon* **35**: 215–230.
- Stute M, Forster M, Frischkom H, Serejo A, Clark J, Schlosser P, Broecker W, Bonani G. 1995. Cooling of tropical Brazil (5°C) during the Last Glacial Maximum. *Science* **269**: 379–383.
- Sun DZ, Lindzen RS. 1993. Distribution of tropical tropospheric water vapor. *Journal of the Atmospheric Sciences* **50**: 1643–1660.
- Talbot RW, Andreae MO, Andreae TW, Harriss RC. 1988. Regional aerosol chemistry of the Amazon Basin during the dry season. *Journal of Geophysical Research* **93**: 1499–1508.
- Taljaard JJ. 1972. Synoptic meteorology of the Southern Hemisphere. In *Meteorology of the Southern Hemisphere*, Newton CW (ed.). Meteorological Monograph **13**, American Meteorological Society: Boston, MA; 139–213.
- Taylor KC, Lamorey GW, Doyle GA, Alley RB, Grootes PM, Mayewski PA, White JWC, Barlow LK. 1993. The 'flickering switch' of late Pleistocene climate change. *Nature* **361**: 432–436.
- Thompson LG, Mosley-Thompson E. 1981. Microparticle concentration variations linked with climatic change: evidence from polar ice cores. *Science* **212**: 812–815.
- Thompson LG, Mosley-Thompson E, Morales Arnao BM. 1984a. Major El Niño/Southern Oscillation events recorded in stratigraphy of the tropical Quelccaya Ice Cap. *Science* **226**: 50–52.
- Thompson LG, Mosley-Thompson E, Grootes P, Pourchet M. 1984b. Tropical glaciers: potential for paleoclimatic reconstruction. *Journal of Geophysical Research* **89**: 4638–4646.
- Thompson LG, Mosley-Thompson E, Bolzan JF, Koci BR. 1985. A 1500 year record of tropical precipitation recorded in ice cores from the Quelccaya Ice Cap, Peru. *Science* **229**: 971–973.
- Thompson LG, Mosley-Thompson E, Dansgaard W, Grootes PM. 1986. The 'Little Ice Age' as recorded in the stratigraphy of the tropical Quelccaya ice cap. *Science* **234**: 361–364.
- Thompson LG, Davis M, Mosley-Thompson E, Liu K. 1988. Pre-Incan agricultural activity recorded in dust layers in two tropical ice cores. *Nature* **336**: 763–765.
- Thompson LG, Mosley-Thompson E, Davis M, Bolzan J, Dai J, Gundestrup N, Yao T, Wu X, Xie Z. 1989. Holocene-Late Wisconsin Pleistocene climatic ice core records from Qinghai-Tibetan Plateau. *Science* **246**: 474–477.
- Thompson LG, Mosley-Thompson E, Davis ME, Bolzan JF, Dai J, Klein L, Gundestrup N, Yao T, Wu X, Xie W. 1990. Glacial stage ice-core records from the subtropical Dundee ice cap, China. *Annals of Glaciology* **14**: 288–297.
- Thompson LG, Mosley-Thompson E, Davis M, Lin P-N, Yao T, Dyurgerov M, Dai J. 1993. 'Recent warming': ice core evidence from tropical ice cores with emphasis upon Central Asia. *Global and Planetary Change* **7**: 145–156.
- Thompson LG, Mosley-Thompson E, Davis ME, Lin P-N, Henderson KA, Cole-Dai J, Bolzan JF, Liu K-b. 1995. Late Glacial Stage and Holocene tropical ice core records from Huascarán, Peru. *Science* **269**: 46–50.
- Thompson LG, Yao T, Davis ME, Henderson KA, Mosley-Thompson E, Lin P-N, Beer J, Synal H-A, Cole-Dai J, Bolzan JF. 1997. Tropical climate instability: the last glacial cycle from a Qinghai-Tibetan ice core. *Science* **276**: 1821–1825.
- Thompson LG, Davis ME, Mosley-Thompson E, Sowers TA, Henderson KA, Zagorodnov VS, Lin P-N, Mikhailenko VN, Campen RK, Bolzan JF, Cole-Dai J. 1998. A 25,000 year tropical climate history from Bolivian ice cores. *Science* **282**: 1858–1864.
- Virji H. 1981. A preliminary study of summertime tropospheric circulation patterns over South America estimated from cloud winds. *Monthly Weather Review* **109**: 599–610.
- Vuille M, Hardy DR, Braun C, Keimig F, Bradley RS. 1998. Atmospheric circulation anomalies associated with 1996/1997 summer precipitation events on Sajama Ice Cap, Bolivia. *Journal of Geophysical Research* **103**: 11 191–11 204.
- Webb RS, Rind DH, Lehman SJ, Healy RJ, Sigman D. 1997. Influence of ocean heat transport of the climate of the last glacial maximum. *Nature* **385**: 695–699.
- White JWC, Steig EJ. 1998. Timing is everything in a game of two hemispheres. *Nature* **394**: 717–718.
- Wirrman D, Mourguiart P. 1995. Late Quaternary spatio-temporal limnological variations in the Altiplano of Bolivia and Peru. *Quaternary Research* **43**: 344–354.
- Wolff T, Mulitza S, Arz H, Pätzold J, Wefer G. 1998. Oxygen isotopes versus CLIMAP (18 ka) temperatures: a comparison from the tropical Atlantic. *Geology* **26**: 675–678.